SPECTROSCOPY OF HIGH-REDSHIFT SUPERNOVAE FROM THE ESSENCE PROJECT: THE FIRST FOUR YEARS

R. J. Foley[1,2,3], T. Matheson[4], S. Blondin[2,5], R. Chornock[1], J. M. Silverman[1], P. Challis[2], A. Clocchiatti[6], A. V. Filippenko[1], R. P. Kirshner[2], B. Leibundgut[5], J. Sollerman[7,8], J. Spyromilio[5], J. L. Tonry[9], T. M. Davis[10,7], P. M. Garnavich[11], S. W. Jha[12,1,13], K. Krisciunas[14], W. Li[1], G. Pignata[15], A. Rest[16,17], A. G. Riess[18,19], B. P. Schmidt[20], R. C. Smith[17], C. W. Stubbs[2,16], B. E. Tucker[20], and W. M. Wood-Vasey[2,21]

Draft version November 26, 2008

ABSTRACT

We present the results of spectroscopic observations from the ESSENCE high-redshift supernova (SN) survey during its first four years of operation. This sample includes spectra of all SNe Ia whose light curves were presented by Miknaitis et al. (2007) and used in the cosmological analyses of Davis et al. (2007) and Wood-Vasey et al. (2007). The sample represents 273 hours of spectroscopic observations with 6.5–10-m-class telescopes of objects detected and selected for spectroscopy by the ESSENCE team. We present 174 spectra of 156 objects. Combining this sample with that of Matheson et al. (2005), we have a total sample of 329 spectra of 274 objects. From this, we are able to spectroscopically classify 118 Type Ia SNe. As the survey has matured, the efficiency of classifying SNe Ia has remained constant while we have observed both higher-redshift SNe Ia and SNe Ia farther from maximum brightness. Examining the subsample of SNe Ia with host-galaxy redshifts shows that redshifts derived from only the SN Ia spectra are consistent with redshifts found from host-galaxy spectra. Moreover, the phases derived from only the SN Ia spectra are consistent with those derived from light-curve fits. By comparing our spectra to local templates, we find that the rate of objects similar to the overluminous SN 1991T and the underluminous SN 1991bg in our sample are consistent with that of the local sample. We do note, however, that we detect no object spectroscopically or photometrically similar to SN 1991bg. Although systematic effects could reduce the high-redshift rate we expect based on the low-redshift surveys, it is possible that SN 1991bg-like SNe Ia are less prevalent at high redshift.

Subject headings: distance scale – galaxies: distances and redshifts – supernovae: general

Electronic address: rfoley@cfa.harvard.edu

[1] Department of Astronomy, University of California, Berkeley, CA 94720-3411.

[2] Harvard-Smithsonian Center for Astrophysics, 60 Garden Street, Cambridge, MA 02138.

[3] Clay Fellow.

[4] National Optical Astronomy Observatory, 950 North Cherry Avenue, Tucson, AZ 85719-4933.

[5] European Southern Observatory, Karl-Schwarzschild-Strasse 2, D-85748 Garching, Germany.

[6] Pontificia Universidad Católica de Chile, Departamento de Astronomía y Astrofísica, Casilla 306, Santiago 22, Chile.

[7] Dark Cosmology Centre, Niels Bohr Institute, University of Copenhagen, Juliane Maries Vej 30, DK-2100 Copenhagen Ø, Denmark.

[8] Department of Astronomy, Stockholm University, AlbaNova, 10691 Stockholm, Sweden.

[9] Institute for Astronomy, University of Hawaii, 2680 Woodlawn Drive, Honolulu, HI 96822.

[10] Department of Physics, University of Queensland, QLD, Australia 4072.

[11] Department of Physics, University of Notre Dame, 225 Nieuwland Science Hall, Notre Dame, IN 46556-5670.

[12] Department of Physics and Astronomy, Rutgers, the State University of New Jersey, 136 Frelinghuysen Road, Piscataway, NJ 08854.

[13] Kavli Institute for Particle Astrophysics and Cosmology, Stanford Linear Accelerator Center, 2575 Sand Hill Road, MS 29, Menlo Park, CA 94025.

[14] Department of Physics, Texas A&M University, College Station, TX 77843-4242.

[15] Departamento de Astronomia, Universidad de Chile, Casilla 36-D, Santiago, Chile.

[16] Department of Physics, Harvard University, 17 Oxford Street, Cambridge, MA 02138.

[17] National Optical Astronomy Observatory / Cerro Tololo Inter-American Observatory, Casilla 603, La Serena, Chile.

[18] Space Telescope Science Institute, 3700 San Martin Drive, Baltimore, MD 21218.

[19] Johns Hopkins University, 3400 North Charles Street, Baltimore, MD 21218.

[20] The Research School of Astronomy and Astrophysics, The Australian National University, Mount Stromlo and Siding Spring Observatories, via Cotter Road, Weston Creek, PO 2611, Australia.

[21] Department of Physics and Astronomy, University of Pittsburgh, 100 Allen Hall, Pittsburgh, PA 15260.

1. INTRODUCTION

A decade after the observations of high-redshift Type Ia supernovae (SNe Ia) caused a sea change in cosmology, indicating that the expansion rate of the Universe is currently accelerating (Riess et al. 1998; Perlmutter et al. 1999) (see Filippenko 2005 for a review), we are still far from understanding the nature of the "dark energy" that causes this accelerated expansion. Recent high-redshift SN Ia surveys, using the large and normalized peak luminosities of SNe Ia, have focused on measuring the equation-of-state parameter of the dark energy, $w = P/(\rho c^2)$, currently constraining it to $\sim 10\%$ (Astier et al. 2006; Riess et al. 2007; Wood-Vasey et al. 2007; Kowalski et al. 2008).

The determination of the expansion history of the Universe with SNe Ia is performed by measuring the luminosity distance as a function of redshift. A relationship between the light-curve shape of a SN Ia and its luminosity is used to obtain precise luminosity distances (e.g., Phillips 1993; Jha et al. 2007; Guy et al. 2007). The

redshift of the object is typically found through spectroscopy of the SN by cross-correlating with low-redshift template spectra or its host galaxy. Although photometry alone can be powerful (e.g., Barris & Tonry 2004; Poznanski et al. 2007), only spectroscopy can currently provide the accurate classification and redshifts necessary for estimating cosmological parameters.

Besides providing the redshift for each object, spectroscopy allows detailed studies of the physics of high-redshift SNe Ia. A critical aspect of high-redshift SN Ia surveys is to only include SNe Ia, and not other transient objects, in their final analysis. Since the optical spectra of SNe Ia are distinct from most transient phenomena, spectroscopy provides a consistent and precise method for determining the nature of each transient (see Filippenko 1997, for a review of SN spectroscopy). Furthermore, with high-redshift SN Ia spectra one can compare physical properties of the objects with their low-redshift counterparts (e.g., Blondin et al. 2006; Balland et al. 2007; Garavini et al. 2007; Bronder et al. 2008; Ellis et al. 2008; Foley et al. 2008).

In order to measure w to $\lesssim 10\%$, the Equation of State: SupErNovae trace Cosmic Expansion (ESSENCE) team has concluded a six-year NOAO survey project using the CTIO 4 m telescope and the MOSAIC II camera with the intention of discovering and following ~ 200 SNe Ia over the redshift range of $0.2 < z < 0.8$ (Miknaitis et al. 2007). During the first four years of the ESSENCE survey, which observed approximately October through December, several hundred transient objects were detected (Miknaitis et al. 2007). As most of these objects were relatively faint ($R > 21$ mag), a large amount of telescope time at 6.5–10 m telescopes was required for spectroscopic follow-up observations. Despite being awarded approximately 100 nights at these facilities over the first four years of the survey, we were still not able to obtain a spectrum of every candidate object (Matheson et al. 2005).

However, during the first 12 search months (ESSENCE searched three months per year), we were able to classify 121 SNe Ia. In this paper, we present the spectra of all spectroscopic targets observed during the first four years of the ESSENCE survey. This sample, which updates and supersedes the analysis of Matheson et al. (2005) for the spectroscopy of the first two years of the ESSENCE survey, includes all SNe Ia presented by Miknaitis et al. (2007) and used in the analysis of Wood-Vasey et al. (2007) and Davis et al. (2007). We discuss our observations in § 2. The classification scheme presented by Matheson et al. (2005), Miknaitis et al. (2007), and Blondin & Tonry (2007) is updated in § 3 (the method is similar to that presented by Miknaitis et al. 2007). In § 4, we discuss the properties of our sample, and we summarize our conclusions in § 5.

2. OBSERVATIONS

Over the first four years of the ESSENCE survey, we detected several thousand transient objects. Since we did not have adequate observing time at large telescopes to follow each transient spectroscopically, we prioritized the objects by a combination of likelihood to be a SN Ia, observational ease, and, occasionally, likely redshift and phase relative to maximum light. These criteria were all determined from our search images, using features such as color and offset from the host galaxy. In particular, the likelihood of an object being a SN Ia is deduced from an approximate photo-z of its host, its $R - I$ color (Tonry et al. 2003), and its rise time. Objects which had particularly blue colors were considered more likely to be core-collapse SNe, while objects with a slow rise time were more likely to be active galactic nuclei (AGNs) or other transients. Further details about the target selection can be found in Matheson et al. (2005) and Miknaitis et al. (2007).

Spectroscopic observations of ESSENCE targets were obtained at a wide variety of telescopes: the Keck I and II 10 m telescopes, the European Southern Observatory 8.2 m Very Large Telescope (ESO VLT), the Gemini North and South 8 m telescopes, the Magellan Baade and Clay 6.5 m telescopes, and the MMT 6.5 m telescope. The spectrographs used were LRIS (Oke et al. 1995) with Keck I, DEIMOS (Faber et al. 2003) with Keck II, FORS1 (Appenzeller et al. 1998) with the VLT, GMOS (Hook et al. 2004) with Gemini (North and South), IMACS (Dressler et al. 2006) with Baade, LDSS2 (Allington-Smith et al. 1994) and LDSS3[1] with Clay, and the Blue Channel (Schmidt et al. 1989) with MMT. Nod-and-shuffle techniques (Glazebrook & Bland-Hawthorn 2001) were used with GMOS (North and South) and some IMACS observations to improve sky subtraction in the red portion of the spectrum. A single spectrum was obtained with the FAST spectrograph (Fabricant et al. 1998) mounted on the Tillinghast 1.5 m telescope at the F. L. Whipple Observatory.

Standard CCD processing and spectrum extraction were accomplished with IRAF[2]. Most of the data were extracted using the optimal algorithm of Horne (1986); for the ESO VLT data, an alternative extraction method based on Richardson-Lucy restoration (Blondin et al. 2005) was employed. Low-order polynomial fits to calibration-lamp spectra were used to establish the wavelength scale. Small adjustments derived from night-sky lines in the object frames were applied. We employed our own IDL routines to flux calibrate the data and remove telluric lines using the well-exposed continua of the spectrophotometric standards (Wade & Horne 1988; Foley et al. 2003).

The photometric data were obtained on the NOAO Blanco 4 m telescope with the MOSAIC II imaging camera. The light curves for the SNe Ia are available online[3] (Miknaitis et al. 2007).

In Table 3, we present a full list of our observations (date of observation, telescope/instrument, and exposure times). We also include information about the nature of each object (object classification, redshift, and, if a SN Ia, phase and light-curve shape). We present the spectra from 2004 and 2005 in Figures 1–6 (*All additional spectra are available in the online edition*). For each SN Ia, we plot both the spectrum of the SN as well as the best-fit SNID (Blondin & Tonry 2007) template
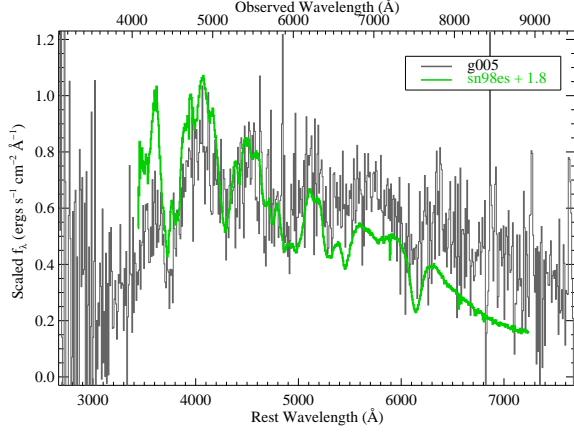
FIG. 1.— Spectrum of g005 at $z = 0.20$ compared to SN 1998es, a SN 1991T-like SN Ia, at $t = 1.8$ d relative to B-band maximum. Differences in the continuum shape are ignored by SNID, which removes a pseudo-continuum from the spectra before cross-correlation.
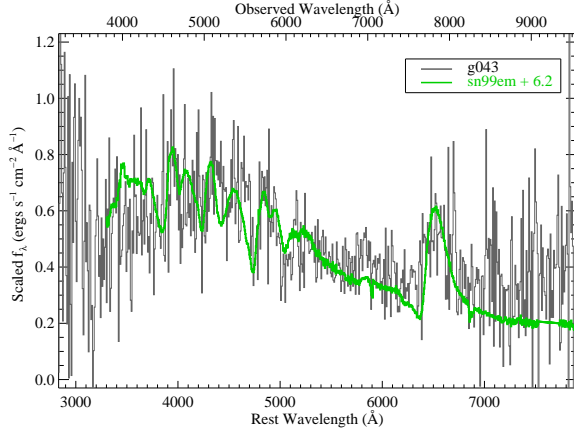
FIG. 2.— Spectrum of g043 at $z = 0.187$ compared to SN 1999em, a SN II-P. Differences in the continuum shape are ignored by SNID, which attempts to remove a pseudo-continuum by fitting a low-order polynomial to the spectra before cross-correlation.
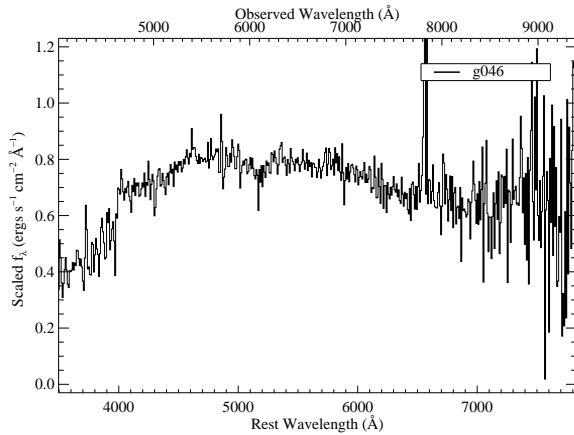
FIG. 3.— Spectrum of g046 at $z = 0.184$. The spectrum is dominated by galaxy light with no detectable amount of light from a transient object.

spectrum.
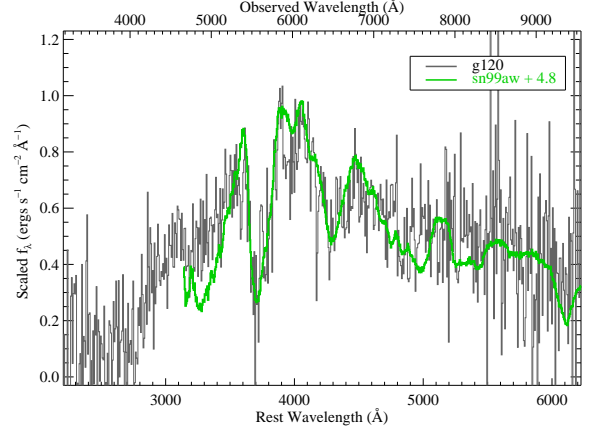
FIG. 4.— Spectrum of g120 at $z = 0.51$ compared to SN 1999aw, a SN Ia, at $t = 4.8$ d relative to B maximum. We were unable to determine a subtype for g120. Differences in the continuum shape are ignored by SNID, which attempts to remove a pseudo-continuum by fitting a low-order polynomial to the spectra before cross-correlation.
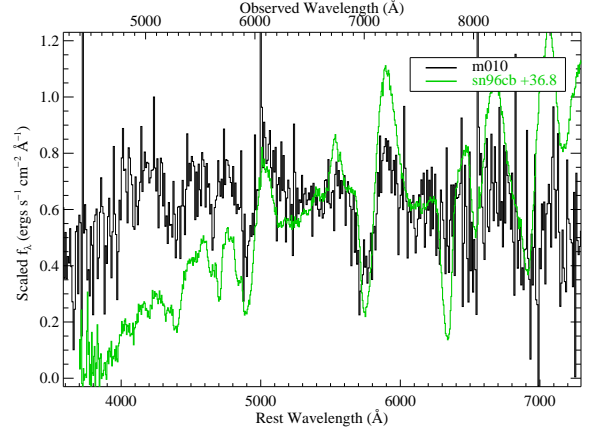
FIG. 5.— Spectrum of m010 at $z = 0.216$ compared to SN 1996cb, a SN IIb. Differences in the continuum shape are ignored by SNID, which attempts to remove a pseudo-continuum by fitting a low-order polynomial to the spectra before cross-correlation.
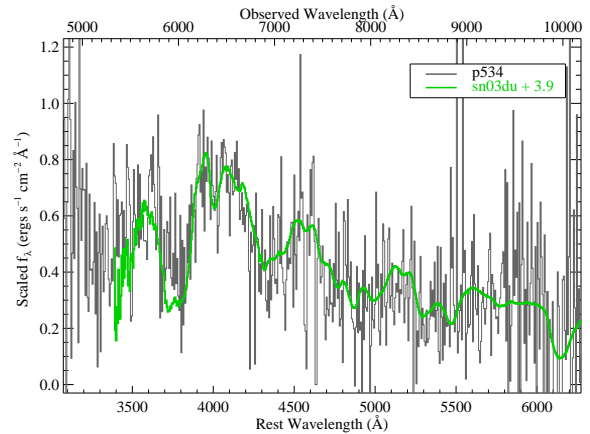
FIG. 6.— Spectrum of p534 at $z = 0.621$ after galaxy subtraction from the superfit routine compared to SN 2003du, a SN Ia. Differences in the continuum shape are ignored by SNID, which removes a pseudo-continuum from the spectra before cross-correlation. Additional figures for all objects listed in Table 3 can be found in the online edition.

3. OBJECT CLASSIFICATION

As all cosmological results resulting from the ESSENCE survey depend on having an uncontaminated sample of SNe Ia, we must pay particular attention to proper object classification. SN classification is based on the optical spectrum (Filippenko 1997; Turatto 2003). Type II SNe are characterized by the presence of obvious hydrogen lines, while Type I SNe lack hydrogen. Type I SNe are further distinguished by the presence of He (Type Ib), strong Si II $\lambda6355$ (Type Ia), or the lack (or weak presence) of both (Type Ic). The velocity of the SN ejecta causes the features to be blueshifted, with the Si II $\lambda6355$ feature typically being observed in absorption at $\sim$6150 Å.

With fully calibrated spectra, we can attempt to classify the object by physical origin. SNe, having broad ($\sim$10,000 km s^{-1}) spectral features, are very distinct from AGNs, galaxies, stars, and other astrophysical objects. However, it can occasionally be difficult to distinguish among SN types. High-redshift SN spectra typically have low signal-to-noise ratio (S/N) and considerable host-galaxy contamination, while lacking the Si II $\lambda6355$ feature (which is redshifted outside the optical range), which can make differentiating between SN types quite difficult. Accordingly, we have implemented the SNID algorithm (Blondin & Tonry 2007) to determine SN types.

SNID correlates an input spectrum with a large database of template spectra at zero redshift. These include nearby ($z < 0.1$) SNe of all types (Ia, Ib, Ic, II), as well as galaxies, AGNs, luminous blue variables (LBVs), and other variable stars (see Blondin & Tonry 2007, for the complete database listing). The SNID algorithm has been extensively described by Blondin & Tonry (2007) and already used to determine the type, redshift, and age of ESSENCE SN spectra by Matheson et al. (2005) and Miknaitis et al. (2007), and we refer the reader to these papers for more details (in particular for what is meant by a "good" correlation).

We also attempt to further divide each SN type into subtypes as follows: Ia — Ia-norm, Ia-pec, Ia-91T, Ia-91bg; Ib — Ib-norm, Ib-pec, IIb; Ic — Ic-norm, Ic-pec, Ic-broad; II — IIP, II-87A, IIL, IIn, IIb. "Norm" and "pec" subtypes are used to identify the spectroscopically "normal" and "peculiar" SNe of a given type (see Blondin & Tonry 2007, for a detailed description of each subtype). For SNe Ia, "91T" indicates spectra that resemble those of the overluminous SN 1991T (Filippenko et al. 1992b; Phillips et al. 1992), and also includes SN 1999aa-like objects (Strolger et al. 2002; Garavini et al. 2004); "91bg" indicates spectra that resemble those of the subluminous SN 1991bg (Filippenko et al. 1992a; Leibundgut et al. 1993), and includes all subluminous objects characterized by a stronger Si II $\lambda5800$ line (e.g., SN 1999gh; Matheson et al. 2008). The spectra that correspond to the "Ia-pec" category in this case are those of SN 2000cx-like (Li et al. 2001a) and SN 2002cx-like (Li et al. 2003) events. These classifications correspond roughly to the categories defined by Branch et al. (1993). For Type Ic SNe, "Ic-broad" is used to identify broad-lined SNe Ic (often referred to as "hypernovae" in the literature; see Galama et al. 1998 and Foley et al. 2003 for well-known

examples), some of which are associated with gamma-ray bursts. The notation adopted for the Type II subtypes is commonly used in the literature. Note that Type IIb SNe (whose spectra evolve from a Type II to a Type Ib, as in SNe 1987K and 1993J — see Filippenko 1988, Filippenko et al. 1993, and Matheson et al. 2000) are included both in the "Ib" and "II" types. All non-SN templates are grouped in the "NotSN" type. We are unable to determine a specific subtype for many objects.

We classify the input spectra in a similar manner to that outlined by Miknaitis et al. (2007). More specifically, we execute four SNID runs to separately determine the type, subtype, redshift, and age of the input spectrum, as follows.

1. **Type:** The input spectrum is asserted to be of a given type when the fraction of "good" correlations that correspond to this type exceeds 50%. In addition, we require the best-match SN template to be of the same type. When the redshift is known beforehand (from narrow emission or absorption lines associated with the host galaxy), we force SNID to only look for correlations at this redshift (±0.02). If SNID determines the type of the input spectrum, an attempt is made to determine its subtype.

2. **Subtype:** To determine the subtype we only consider "good" correlations with template spectra corresponding to the previously determined type. The input spectrum is asserted to be of a given subtype when the fraction of "good" correlations that correspond to this subtype exceeds 50%. In addition, we require the best-match SN template to be of the same subtype. Examples of SNe Ia for which we could and could not determine a subtype are g005 (displayed in Figure 1) and g120 (displayed in Figure 4, respectively. Again, we use the galaxy redshift when available. Regardless of whether SNID determines a subtype, a third run is executed to determine the redshift.

3. **Redshift:** The SNID redshift corresponds to the median of all "good" template redshifts, while the redshift error is given as the standard deviation of these same redshifts (see Blondin & Tonry 2007, for more details). If a subtype has been determined, we only consider "good" correlations with template spectra corresponding to this subtype; otherwise, all template spectra of the given type are used. Here no prior information on the galaxy redshift is used. If a redshift is determined in this run, a fourth run is executed to determine the age.

4. **Age:** The SNID age corresponds to the median of all "good" template ages, while the age error is given as the standard deviation of these same ages. If a subtype has been determined, we only consider "good" correlations with template spectra corresponding to this subtype; otherwise, all template spectra corresponding to the given type are used (as for the redshift determination). The redshift is fixed to the host-galaxy redshift when available, or to the previously determined SNID redshift otherwise (±0.02). Blondin & Tonry (2007) mention that the age error calculated this way is typi-

cally overestimated, but here we make no attempts to compute a more robust age error (as done by Blondin et al. 2008).

Note that we have run SNID on *all* ESSENCE spectra, but only report the SNID output for spectra classified as SNe (Table 3). For all other spectra, we rely on the visual classification by spectroscopy experts within our team. In a few cases, a spectrum not classified as a SN Ia by SNID is found to be consistent with a SN Ia spectrum through visual inspection. For these cases we report a "Ia?" classification. In fact, SNID can sometimes fail to correctly classify an input SN Ia spectrum, mainly because of low S/N or excessive galaxy contamination. Blondin & Tonry (2007) showed that the redshift and age determination with SNID is greatly affected for input spectra that consist of more than 50% galaxy light.

In addition to using SNID, we have applied an alternate technique for SN classification that is based on a χ^2 minimization of fitting a SN spectrum to template spectra with a variable extinction and galaxy contamination (Howell et al. 2005). This method is implemented in the `superfit` IDL package. The main advantage of the χ^2 minimization technique is that it can classify SNe from spectra that are highly contaminated by galaxy light. One of the main drawbacks of `superfit` is that it assumes that the continuum of a high-redshift SN Ia must be similar to that of a low-redshift SN Ia. Although usually this can be worked around by having a different value for the extinction (which will change the continuum shape of the spectrum even if the value of the "extinction" is not strictly physical) or a different galaxy template, there is the possibility that `superfit` will not classify some objects that SNID does. This is demonstrated by n404 in Figure 7. For this object, SNID classifies it as a SN Ia at $z = 0.211$. For the same object, `superfit` classifies it as a SN II, with 3 of the top 5 matches with low-redshift template spectra being SNe II. The best-fit SN Ia template places n404 at $z = 0.07$. One has to go to the eighth-best match to obtain a SN Ia at the same redshift as SNID. Having performed a "brute-force," where we did not carefully adjust various parameters to achieve the best results for each spectrum, classifcation for all spectra in our sample, we found other object in our sample where SNID and `superfit` differ. However, a more careful `superfit` analysis may have very few discrepancies with SNID. The other main drawback of `superfit` is that although `superfit` produces a χ^2-like goodness-of-fit parameter, there is no formal evaluation of the uncertainty of any of the derived values (cf, the redshift error in SNID is related to the height of the correlation peak; see Blondin & Tonry 2007).

Applying the χ^2 minimization technique to all spectra which were not originally classified by SNID, we obtained several candidate SNe. The `superfit` package will output a galaxy-subtracted spectrum using a galaxy fraction (and galaxy type) that best matches a given SN template spectrum. Since we have not modeled the robustness of the goodness-of-fit parameter from this technique, we attempted to classify the galaxy-subtracted spectra with SNID. We fit the top five galaxy-subtracted `superfit` spectra with SNID, looking for a consensus result. For 99 potential candidates, this process yielded one additional SN Ia? (f123), as well as identifying a second-
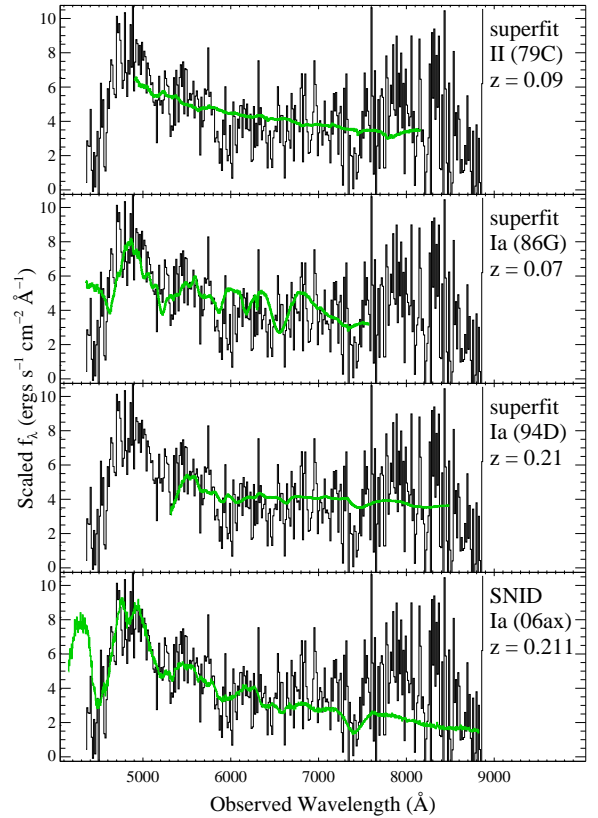
FIG. 7.— Observed spectrum of ESSENCE SN n404. The green lines are low-redshift comparison spectra. The top three panels show the first (SN II 1979C at $z = 0.09$), fourth (first SN Ia; SN 1986G at $z = 0.07$), and eighth (first SN Ia at $z \approx 0.21$; SN 1994D) best-matched low-redshift template spectra from `superfit` in green. The bottom panel shows the best-matched low-redshift template spectrum from SNID in green. Differences in the continuum shape are ignored by SNID, which removes a pseudo-continuum from the spectra before cross-correlation; therefore, the continuum of the SNID template may not exactly match that of n404.

epoch spectrum of a SN Ia (p534; as identified from the other spectrum by SNID) as a SN Ia.

There is some concern that extra degrees of freedom are introduced into our SNID fitting as the `superfit` packages changes the spectrum by applying an extinction estimate and removing a galaxy spectrum from each input spectrum. However, since SNID normalizes all spectra to have a flat continuum, it is relatively insensitive to reddening.

We have already shown the excellent agreement between the SNID correlation redshift and the redshift of the SN host galaxy (when known) in several publications (Matheson et al. 2005; Miknaitis et al. 2007; Blondin & Tonry 2007; Blondin et al. 2008). Figure 8 again shows that the SNID redshifts agree well with the host-galaxy redshifts, with a dispersion about the one-to-one correspondence of only ∼0.006. This figure contains only the SNe Ia where we have an independent measurement of the redshift from a galaxy spectrum.

The template spectra in the SNID database have ages corrected for the $1/(1 + z)$ time-dilation factor expected in an expanding universe (e.g., Blondin et al. 2008), such that SNID determines ages in the SN rest frame. No correction to the age for light-curve width has been made. We can then compare these age estimates ($t_{\rm SNID}$)
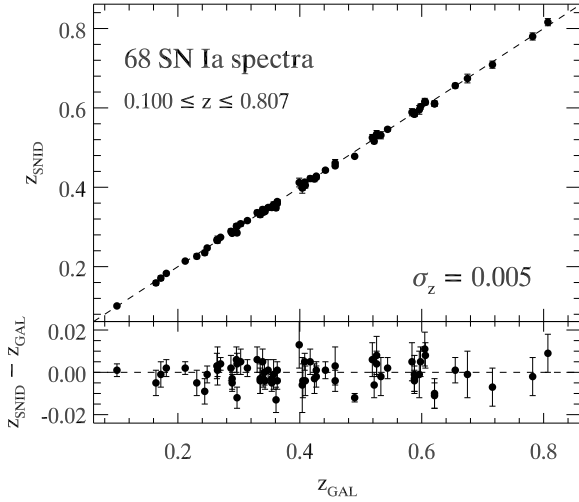
FIG. 8.— Comparison of redshifts determined from cross-correlations with SN Ia spectral templates using SNID ($z_{\rm SNID}$) and from narrow lines in the host-galaxy spectrum ($z_{\rm GAL}$; *upper panel*). We show the residuals *vs.* $z_{\rm GAL}$ in the lower panel.

with those inferred from a well-sampled light curve (see Miknaitis et al. 2007). We expect a one-to-one correspondence between the light-curve rest-frame age,

$$t_{\rm LC} = \frac{\Delta t_{\rm obs}}{1 + z}, \qquad (1)$$

and $t_{\rm SNID}$, where $\Delta t_{\rm obs}$ is the time difference (in the *observer* frame) between maximum light and the time the spectrum was obtained.

The result is shown in Figure 9. We use all objects with a good light-curve fit and a good SNID age, resulting in a total of 59 SN Ia spectra with rest-frame light-curve ages in the range $-11.0 \leq t_{\rm LC} \leq 19.4$ d. The dispersion about the $t_{\rm SNID} = t_{\rm LC}$ line is $\sigma_t \approx 2.4$ d, similar to what was found by Blondin & Tonry (2007). We show the residuals versus $t_{\rm LC}$ in the lower plot. The mean residual is approximately -0.7 d. Two points at $t_{\rm LC} < -10$ d are $\sim 2\sigma$ off the null residual line; this is due to the low number of SN Ia templates at these early phases.

The fact that the SNID correlation redshift and age measurements agree so well with the galaxy redshifts and light-curve ages, respectively, is a strong argument in favor of the similarity of these SNe Ia with local counterparts. This further confirms the results of Matheson et al. (2005), who found that our classification techniques were robust and saw no major indications of SN Ia evolution in our sample. Foley et al. (2008) also see this for the overall sample.

4. HIGH-REDSHIFT SAMPLE

Over the four seasons, we obtained 329 spectra of 274 objects for a total of 273 hours of integration. This has yielded 118 SNe Ia, 9 SNe Ia?, 16 SNe II, 7 SNe Ib/c, 56 galaxies (which may have some SN light in the spectrum, but at an undetectable level), 20 AGNs, 4 stars, and 44 unidentified objects. We provide a detailed assessment of our object classification in Table 1.

Objects with no definitive SNID classification or obvious "by-eye" classification are labeled as "Unk." Objects with no signal in their spectra are labeled as "N.S." Together, objects with these classifications compose the subsample of unidentified objects.
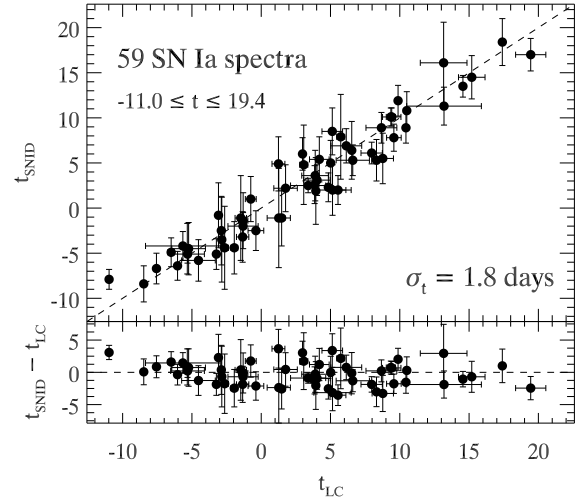
FIG. 9.— Comparison of SN spectral ages determined using SNID ($t_{\rm SNID}$) and rest-frame light-curve ages ($t_{\rm LC}$) of high-z SNe Ia (*upper panel*). We show the residuals vs. $t_{\rm LC}$ in the lower plot.

TABLE 1
ESSENCE SPECTROSCOPY RESULTS: THE FIRST 4
YEARS

Type	Year 1	Year 2	Year 3	Year 4	Total
Ia	15	35	30	38	118
Ia?	0	3	2	4	9
II	1	2	6	7	16
Ib/c	1	2	2	2	7
AGN	3	9	0	8	20
Gal	8	11	20	17	56
Star	2	2	0	0	4
Unk/N.S.	6	17	13	8	44
Total	36	81	73	83	274

NOTE. — Since there were no template observations obtained before Year 1 and no long baseline observations to easily reject AGNs and variable stars, there were fewer high-quality SN Ia candidates in Year 1. As a result, Year 1 had fewer SNe Ia confirmed compared to later years.

For several objects, we have changed our classification from that published by Matheson et al. (2005). This is mostly the result of an improved version of SNID and additional low-redshift templates for comparison. Additionally, the `superfit` routine provided several classifications that we were not previously able to determine. In Table 2, we list the objects with different classifications between Matheson et al. (2005) and this work, as well as the dominant reason for the reclassification.

4.1. Survey Efficiency

In order to meet our goal of ~ 200 SNe Ia over six years, we tried to use our resources as efficiently as possible to detect and classify SNe Ia. Although the ESSENCE survey has been completed, performing an analysis of the efficiency of ESSENCE will provide useful information for the planning of future surveys (e.g., Pan-STARRS and DES).

The process of detecting and classifying SNe Ia can be separated into two tasks: pre-selecting potential candidates so SNe Ia represent a high percentage of spectroscopic targets, and properly classifying the spectrum of a SN Ia as a SN Ia. The first task is based solely on parameters derived from imaging. The second task relies on

TABLE 2
ESSENCE OBJECT RECLASSIFICATION

ESSENCE ID	IAUC ID	Matheson et al. (2005) Classification	The Paper Classification	Notes
c016.wxm1_04	⋯	AGN	Gal	
c022.wxu2_15	⋯	II?	Ib	IIb subtype
d009.waa6_16	⋯	Gal	Ia	
d120.wcc1_2	⋯	⋯	AGN	Not listed by Matheson et al. (2005)
e141.wdd7_2	⋯	II	Ib	IIb subtype
e143.wdd7_3	⋯	II	Ib	
e149.wdd5_10	2003ks	Ia?	Ia	
f001.wbb7_1	2003kv	Unk	II	
f044.wbb8_8	⋯	Gal	Ia	
f123.wcc1_7	⋯	Gal	Ia?	
f221.wcc4_14	2003lk	Ia?	Gal	
f301.wdd6_1	⋯	Ia?	Ia	
f308.wdd6_10	⋯	Ia?	Ia	

having a method of classifying events with high accuracy (such as the SNID algorithm) and having spectra of sufficient quality for that method to determine a classification (which depends on observing conditions, separation from the host galaxy, brightness of the target, exposure time, the spectrograph's wavelength range, etc.).

To examine the synergy of our search with the large-aperture telescope time we used for spectroscopy, we present histograms of our redshift distribution and phase of the first spectrum of each SN Ia in Figures 10 and 11, respectively. From these figures we see that as the survey matured, we were able to detect higher-redshift objects with greater efficiency. The SNe Ia detected during the first two years have an average redshift of 0.38 (and median redshift of 0.41), while the SNe Ia detected during years 3 and 4 have an average redshift of 0.45 (and median redshift of 0.42). We also detected 7 (21) SNe Ia with $z > 0.7$ ($z > 0.6$) in the second two years, while we had detected none (4) in the first two years. Moreover, we were able to detect, observe, and classify SNe Ia at later phases after maximum brightness, when the SNe are fainter.

Figure 12 shows that for objects with larger Δ^4 (corresponding to being less luminous), we only obtain spectra near maximum light, while for objects with smaller Δ (corresponding to being more luminous), we obtain spectra for a wide range of phases. Besides being less luminous, high-Δ SNe Ia fade faster than low-Δ SNe Ia, making high-Δ SNe Ia become even fainter relative to low-Δ SNe Ia the farther they are from maximum light. Both of these biases (faintness and faster declining) for high-Δ objects are expected for our sample. However, one may argue that since there are fewer total spectra obtained for older SNe we may be seeing a manifestation of small-number statistics as opposed to a selection effect. To test this hypothesis, we performed a Kolmogorov-Smirnov (K-S) test on the objects with $|t| < 5$ d compared to those with $5 < t < 20$ d and $t > 20$ d; we find the probability that the sets are chosen from different distributions to be 75.6% and 99.9%, respectively. The earlier data are marginally consistent, while the later data are different at a high significance. This is consistent with the expected bias.

In Figure 12, we see that there are 5 SNe (d058,

^{4}　$M_V(t = 0) = -19.504$ mag $+ 0.736\Delta + 0.182\Delta^2 + 5\log_{10}(H_0/65)$ (Jha et al. 2007).
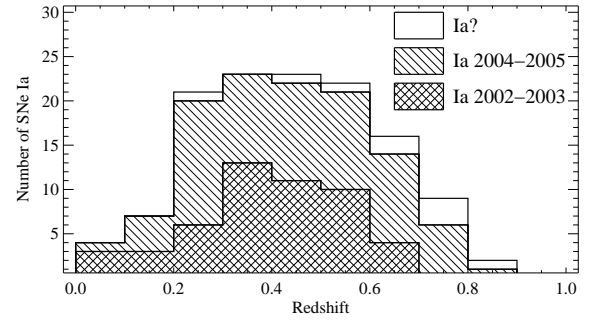
FIG. 10.— Redshift distribution of spectroscopically identified SNe Ia from the first four years of the ESSENCE survey. The SNe for which we have a high confidence of being of Type Ia (as determined by SNID) are plotted in the hashed region. The open region represents SNe for which we have less confidence and have been classified "SNe Ia?."
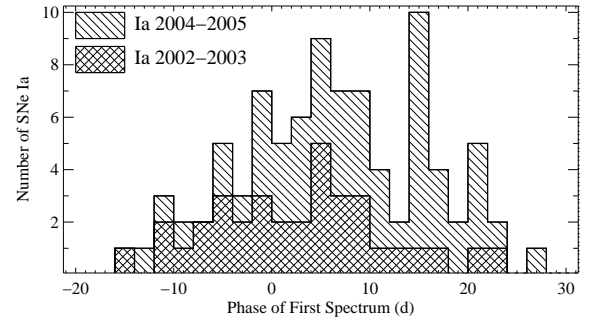
FIG. 11.— Phase (relative to maximum brightness) distribution of spectroscopically identified SNe Ia from the first four years of the ESSENCE survey and light curves fit by Wood-Vasey et al. (2007).

h311, m022, m043, and m057) with $\Delta < -0.4$, the fiducial Δ limit for the multicolor light-curve shape method (MLCS; Riess et al. 1996; Jha et al. 2007) based on the broadest local SN Ia light curves. There are two reasons for such a low value of Δ: the light curve is broader than any local template, or the light curve is of low quality and the MLCS fit is not robust. Of the 5 SNe, three (h311, m022, m057) fail the $\chi^2/$dof < 3 cutoff set by Wood-Vasey et al. (2007). One (m043) has no light-curve points before maximum, so it is difficult to determine if the light curve is truly broad. The final one (d058, with $\Delta = -0.470$) has a well-sampled light curve and is

FIG. 12.— Distribution of measured Δ of ESSENCE SNe Ia vs. phase (relative to maximum brightness). Only objects that had light curves fit by Wood-Vasey et al. (2007) have been plotted. The dashed line indicates the Δ limit beyond which MLCS has to extrapolate to fit light curves. As such, objects with $\Delta < -0.4$ should be discounted.

FIG. 13.— Efficiency of our spectroscopic follow-up observations over the 12 search months in the first four years of ESSENCE. The overall efficiency is 43%.

FIG. 14.— Efficiency of our spectroscopic follow-up observations over the 12 search months in the first four years of ESSENCE as a function of total spectroscopic exposure time in a given month.

likely to be truly broad. Examining the spectrum, it does not appear that d058 is peculiar, however the small rest-frame wavelength range ($\sim3000 - 5000$ Å) prevents an investigation of important lines such as Si II $\lambda6355$. The first four objects should be ignored since their Δ values are likely to be incorrect. The final object, d058, should be discounted. Although Δ is a well-defined quantity for $\Delta < -0.4$ (indicating the width of a light curve), for such values we must extrapolate beyond the local sample, leading to potentially incorrect distance and luminosity measurements.

We further investigate if we are limited in our number of classified SNe Ia by our search or by our usable time on large-aperture telescopes. In Figure 13, we show our efficiency (given by the ratio of SNe Ia classified to total objects we observed) as a function of search month. However, there are many objects where, after a short exposure, we recognized that it was not a SN Ia. An exposure-time weighted efficiency will be higher than that shown in Figure 13. Throughout the first four years, we consistently classified $\sim43\%$ of all spectroscopic targets as SNe Ia, perhaps slightly increasing our efficiency with time.

In Figure 14, we show that our efficiency does not change with the amount of spectroscopic time in a given month. This indicates that for a broad range of the number of transients detected per month in our search or for a broad range of spectroscopic follow-up time in a given month, we would obtain about the same ratio of SNe Ia to total spectroscopic targets.

This result is perhaps a little counterintuitive. There are several factors involved. For example, with infinite potential targets from the search, one expects to be able to properly identify excellent candidate SNe Ia, resulting in a higher efficiency. Similarly, with infinite spectroscopic follow-up time, one expects to be able to obtain a spectrum of every transient, resulting in a lower efficiency. But there are other factors. First, when there was
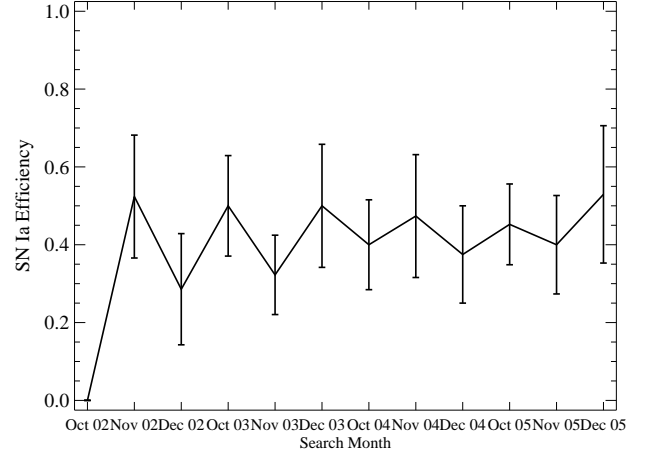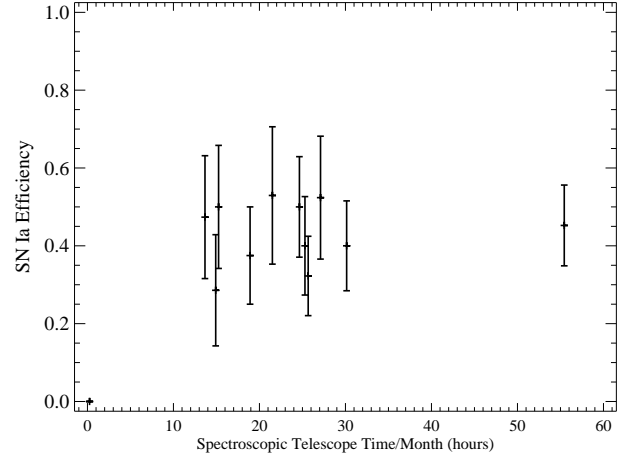
a paucity of potential spectroscopic targets, we would obtain additional spectra of already confirmed SNe Ia rather than observe candidates that had a small possibility of being a SN Ia. Another aspect is the image quality of the search. If a particular month had poor weather or bad seeing at Cerro Tololo, we would typically detect brighter, more isolated objects at lower redshifts. So even if there were fewer objects from which to choose, the objects were typically easier to observe. It is difficult to disentangle all of these effects, but we have shown from our measured efficiencies that they naturally balanced over the first four years of the ESSENCE survey.

Howell et al. (2005) showed that the Supernova Legacy Survey (SNLS) was able to improve their efficiency from 54% to 71% by utilizing multiple colors of the transients and hosts to better predict whether a transient is a SN Ia. The ESSENCE survey, which searched in only R and I, was unable to perform such an analysis. Furthermore, ESSENCE only had R and I photometry for the host galaxies, reducing our ability to determine precise host-
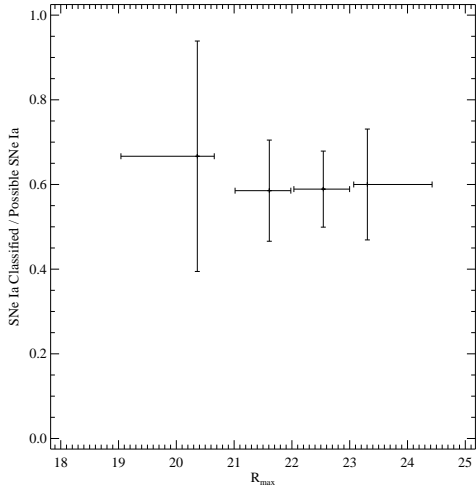
FIG. 15.— Ratio of the number of SNe Ia classified to the number of total objects which may be SNe Ia (those classified as SNe Ia, SNe Ia?, Gal, Unk, or N.S.) as a function of peak R magnitude. The bins are for objects with $R_{max} < 21$, $21 \leq R_{max} < 22$, $22 \leq R_{max} < 23$, and $R_{max} > 23$ mag, with the points plotted at the median value for each bin.

galaxy photo-z values. Obviously, if spectroscopic efficiency is a priority, future surveys should have many-filter observations of transients and host galaxies. Additionally, having multiple colors of SNe Ia will greatly improve the measurement of SN colors and dust extinction, which in turn should improve SN distances.

Although we have been able to reduce the number of persistent transients (AGNs, variable stars) observed spectroscopically, we still observed 7 AGNs in year 4 (compared to 3, 9, and 0 for years 1, 2, and 3). These objects were selected for spectroscopic observation despite some indications that they were AGNs. This can be attributed to a human error, and having more humans vet the candidates would help prevent such future observations.

Finally, if we remove all transients which are definitely not SNe Ia (i.e., those objects that have spectra which identify them as other types of transient objects), we can determine how successful our spectroscopic classification would have been if we had fewer contaminants. Figure 15 shows the ratio of the number of SNe Ia to the number of total objects which may be SNe Ia (those classified as SNe Ia, SNe Ia?, Gal, Unk, or N.S.) as a function of peak R magnitude. This is a measurement that approximates our efficiency if we had better photometric preselection. We do note that for a fixed amount of galaxy-light contamination it is easier to classify a bright SN Ia than a relatively faint SN Ib/c, indicating that the "Gal" category may contain a lower fraction of SNe Ia than the survey as a whole.

Although not all objects classified as Unk, for example, are SNe Ia, this ratio still yields a useful approximation of our spectroscopic efficiency as a function of brightness. Note that the ratio is a minimum efficiency since it will increase by either identifying objects as transients other than SNe Ia (by decreasing the number of possible SNe Ia) or by identifying objects as SNe Ia (by increasing the number of SNe Ia).

Regardless of maximum brightness, we appear to identify similar percentages of possible SNe Ia and definite

SNe Ia. Therefore, we appear to apply a consistent approach to obtaining sufficient-quality spectra to identify SNe Ia for objects of all brightnesses.

4.2. Sample Demographics

In the local universe, there are many subtypes of SNe Ia. The most common peculiar subtypes are those of SNe 1991T and 1991bg (described in Section 3), corresponding to more and less luminous events, respectively. Li et al. (2001b) found that 20% and 16% of nearby SNe Ia are similar to SNe 1991T and 1991bg, respectively. To determine if the ESSENCE sample of SNe Ia is representative of the full SN Ia population and if the high-redshift population has different demographics from the low-redshift population, we examine the peculiarity rate in the ESSENCE sample.

4.2.1. Peculiar Type Ia Supernova Sample

SNID cross-correlates a SN spectrum with a library of template SN spectra. The template spectra have been classified into subtypes (see Section 3). If $> 50\%$ of the best-fit template spectra for a given SN are all part of a particular subtype, then the SN is considered to be of that subtype.

Using SNID, we have determined that five of our SNe Ia (b004, d009, d083, d093, and p534) are SN 1991T-like SNe Ia. Matheson et al. (2005) also claimed that b004 and d083 are similar to SN 1991T. The light curves of b004 and d009 were not fit by Wood-Vasey et al. (2007); however, d083, d093, and p534 were found to have $\Delta = -0.273$, -0.365, and -0.096, respectively. SN 1991T and the SN 1991T-like SN 1999aa have $\Delta = -0.220$ and -0.271, respectively (Jha et al. 2007).

There are an additional 19 objects which do not pass the threshold necessary to be safely considered as a SN 1991T-like object, but have a best-fit template that is of that subtype. For the sample of 24 SNe Ia that are either classified as SN 1991T-like or have a best-fit template of that subtype, there are 16 objects with light curves fit by Wood-Vasey et al. (2007), having a mean Δ of -0.178. The entire ESSENCE sample with light curves fit by Wood-Vasey et al. (2007) has a mean Δ of -0.121. The Δ distributions of both the entire sample and the subsample of SN 1991T-like objects are shown in Figure 16.

We have also identified a single object (m226) with a best-fit template similar to SN 1991bg, but it did not pass the threshold to be considered SN 1991bg-like. Since no SN 1991bg-like objects have been spectroscopically confirmed at high redshift, we pay particular attention to the classification of this object. There are several reasons why we do not believe m226 should be classified as a SN 1991bg-like object. First, the spectrum only matched three SNID template spectra, two of which were SNe Ia-norm. Second, the best-match template spectrum is of SN 1999gh at 42 d past maximum light, while the light-curve age is 24 d past maximum light. The best-match template with a spectral age near that of the light-curve age of m226 is SN 2002bo (at 29 d past maximum light), which is a SN Ia-norm. Third, SN 1999gh is a low-luminosity SN Ia with a deep Si II $\lambda5800$ line; however, it does not share many of the spectral features of SN 1991bg (Matheson et al. 2008). Fourth, the spectrum of m226 has a relatively low S/N ratio, where proper
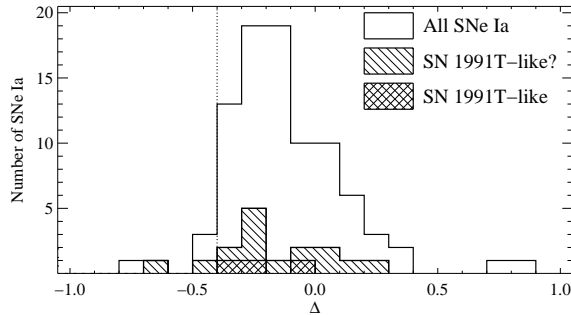
FIG. 16.— Δ distribution of spectroscopically identified SNe Ia from the first four years of the ESSENCE survey and light curves fit by Wood-Vasey et al. (2007). Subsamples of objects identified by SNID as either being of the subtype consisting of SN 1991T-like objects or having a best-fit template of that subtype are also shown. Increasing Δ corresponds to narrower light curves and less luminous SNe Ia. The dotted line indicates the Δ limit beyond which MLCS has to extrapolate to fit light curves. As such, objects with $\Delta < -0.4$ should be discounted.

subtyping is dubious. Finally, the light-curve fit of m226 yielded $\Delta = -0.227$, which is on the opposite end of the Δ range from SN 1991bg-like objects. With all of these data, we are therefore unable to properly classify the subtype of m226.

4.2.2. Peculiarity Rate

The spectral features that distinguish SNe 1991T and 1991bg from SNe Ia-norm can be hidden by low-S/N spectra, spectra with a restricted rest-frame wavelength range, and spectra obtained well after maximum brightness. Nevertheless, we still have observed very few peculiar SNe Ia in the ESSENCE survey. Of the 131 SNe Ia and SNe Ia?, we have spectroscopically confirmed 5 SNe Ia similar to SN 1991T (with 19 additional potential objects). Therefore, we have determined that 4–19% of the SNe Ia from the ESSENCE survey are similar to SN 1991T, while no ESSENCE SN is similar to SN 1991bg. Because of selection effects (discussed below), our upper limit of SN 1991T-like objects may be lower than the real value; however, since the lower limit is determined by definitive detections, it cannot be smaller. Bronder et al. (2008) spectroscopically confirmed 2–3 high-redshift SNLS SNe Ia out of a sample of 54 to be comparable to SN 1991T; this rate is similar to that found in the ESSENCE survey.

Comparing to low-redshift SN searches, Li et al. (2001b) found that 20% and 16% of nearby SNe Ia are similar to SNe 1991T and 1991bg, respectively. Our raw rate of SN 1991bg-like objects appears to be very low compared to the low-redshift rates. However, with a typical limiting magnitude of $R = 24$ mag, we would only expect to be complete for SN 1991bg-like objects out to $z \approx 0.35$. We have detected 46 SNe Ia (or SNe Ia?) with $z \leq 0.35$. If the low-redshift rates are similar to the rates at $z \approx 0.35$, we would expect to have detected 7 SN 1991bg-like SNe Ia in this subsample. If there are no SN 1991bg-like SNe Ia at high redshift, but the ratio of SN 1991T-like to SNe Ia-norm remains constant, then one would expect 24% of high-redshift SNe Ia to be similar to SN 1991T. Considering the selection effects involved, we believe that the rate of SN 1991T-like SNe Ia spectroscopically confirmed in the ESSENCE survey is consistent with the rate found at low redshift.
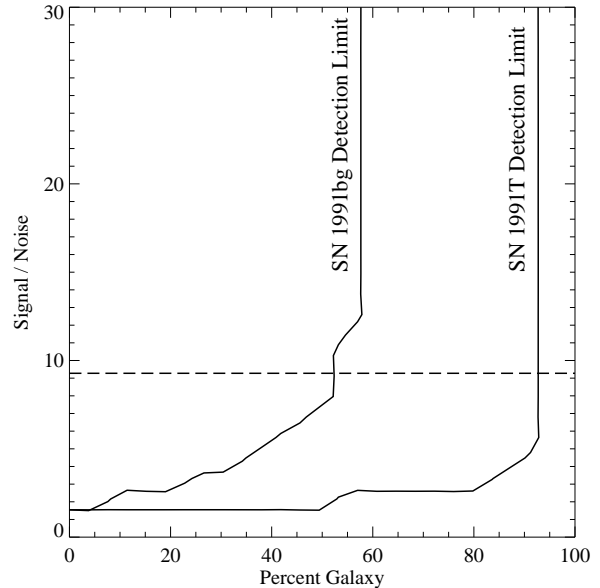
FIG. 17.— Contours representing the region of S/N-galaxy contamination parameter space that SNe Ia similar to SNe 1991T and 1991bg at $z = 0.35$ will have a correct subtype classification from SNID. We have made no assumption about the relative luminosities of the SNe or host galaxies. If a spectrum is to the upper-left of the contour, then it is correctly classified into its subtype. The dashed line is the median S/N for our sample of SNe Ia with $z \leq 0.35$. The detection efficiencies show that we should recover nearly every SN 1991T-like SN Ia to this redshift, while the detection of SN 1991bg-like objects is heavily dependent on the amount of galaxy contamination.

Conversely, we find that the raw rate of SN 1991bg-like SNe Ia found in the ESSENCE survey is low. A further indication of a low raw rate is that no survey has spectroscopically confirmed a SN 1991bg-like SNe Ia at high redshift.

To determine a reasonable detection efficiency for SNe similar to SN 1991bg, we performed a basic simulation. Starting with the maximum-light spectrum of SN 1991bg, we added a varying amount of noise and galaxy contamination (using the spectrum of an elliptical galaxy). We then processed the spectra with SNID, removing SN 1991bg from our sample of template SNe and restricting our wavelength range to 3000–6600 Å, an appropriate rest-frame wavelength for $z = 0.35$. From this, we were able to determine what parameters of S/N and galaxy contamination would yield a correct subtype classification by SNID. We repeated this process for SN 1991T with an Sb galaxy. The results are shown in Figure 17. For this simulation, we did not make any assumption about the SN or host galaxy luminosities. SN 1991bg-like objects should be less luminous and have more luminous host galaxies than SN 1991T-like objects. This would mean that the average spectrum of a SN 1991bg-like object should have more galaxy contamination than that of a SN 1991T-like object.

From Figure 17, we see that for $z \leq 0.35$, we should detect essentially all SN 1991T-like objects. However, for SN 1991bg-like objects, the detection efficiency is strongly dependent on galaxy contamination. We would detect most SN 1991bg-like objects with $< 60\%$ galaxy contamination.

If we assume that the low- and high-redshift peculiar-

ity rates are the same, then selection effects and classification systematics must decrease the SN 1991T-like classification rate by a factor of 1–5. Considering that SN 1991bg-like objects tend to be found in high surface-brightness galaxies, many of these objects will be fainter than their galaxies at their position. We are able to remove a significant amount of galaxy light during spectral reductions (particularly for elliptical galaxies where the radial light distribution is smooth), but it is still likely that a significant number of spectra of these objects would be dominated by galaxy light, and therefore would not be classified in this subtype by SNID.

If we assume that most spectra of SN 1991bg-like objects will have galaxy contaminations of 25–75% and a S/N of 4–15 (similar to most of our spectra), we can determine the percentage of these spectra that SNID would classify as SN 1991bg-like objects. Placing these constraints in the parameter space shown in Figure 17, we see that 54% of the remaining parameter space results in a positive detection.

If we assume that the selection effects and classification systematics are essentially equal to the detection efficiency of SNID given our assumed parameters above, we require a bias factor of 1.86 for the SN 1991bg-like objects compared to the SN 1991T-like objects. Using this factor, we would expect the SN 1991bg-like peculiarity rate to be 2–8% for the ESSENCE sample. This corresponds to 1–4 SNe in our $z \leq 0.35$ sample, consistent with our non-detection of SN 1991bg-like events in our sample. Increasing the sample size and constraining the bias factors will greatly improve the constraints.

A secondary method to examine the rate of SN 1991bg-like objects is by measuring the light-curve shapes of our SNe Ia. SN 1991bg-like objects have significantly different light-curve shapes than normal SNe Ia, with corresponding $\Delta > 1$. Our sample contains 31 SNe Ia with $z \leq 0.35$ and Δ information. If the local rate of SN 1991bg-like objects is constant to $z = 0.35$, then we would expect to have 5 SN 1991bg-like objects in this sample. None of the SNe Ia in this sample have $\Delta > 1$. Assuming that all objects spectroscopically similar to SN 1991bg also have $\Delta > 1$, the nondetection of any of these objects is 2.2σ from the expected value.

A significant bias against classifying SN 1991T-like SNe Ia (particularly objects similar to SN 1999aa) at high redshift is that their post-maximum spectra are very similar to those of SNe Ia-norm. For instance, there is essentially no difference between the spectra of the normal SN 1994D and SN 1999aa one week after maximum brightness (Garavini et al. 2004). Therefore, for a large percentage of our SNe Ia, we have no real constraint on the peculiarity of the individual object. More detailed modeling is necessary to determine the classification success as a function of phase, S/N, and wavelength range of a particular spectrum.

5. CONCLUSIONS

We have presented optical spectra of targets selected for follow-up observations during the first four years of the ESSENCE survey. We have shown that as the survey matured, we were able to detect more SNe Ia at higher redshifts and at later phases without reducing efficiency for a total of 127 SNe Ia and possible SNe Ia ("Ia?"). There were more SNe Ia observed in the second two years

than in the first two years, showing that we are on track to reach the goal of the ESSENCE survey: constraining the equation-of-state parameter of dark energy to $\lesssim 10\%$ by observing ~ 200 SNe Ia over the redshift range $0.2 \lesssim z \lesssim 0.8$.

The spectra of the ESSENCE high-redshift SNe Ia are broadly consistent with those of their low-redshift counterparts; see Foley et al. (2008) for a detailed comparison of composite spectra made from this sample. If the ESSENCE SNe Ia were drastically different from their local counterparts, then the correlations of redshift and age found by SNID would have larger scatter. We are able to automatically classify the majority of our objects using SNID. However, human intervention, through visual inspection or using a second fitting program, was necessary to properly classify several objects. SNID is able to accurately quantify the redshift and phase determination for our sample of SNe Ia. The peculiarity rate of the spectroscopically distinct SN 1991T-like and SN 1991bg-like objects are consistent with low-redshift rates. None of the spectra from our sample or light curves fit by Wood-Vasey et al. (2007) are similar to the spectroscopically peculiar SN 1991bg. However, if we consider systematic effects, these non-detections are consistent with low-redshift rates.

REFERENCES

Allington-Smith, J., Breare, M., Ellis, R., Gellatly, D., Glazebrook, K., Jorden, P., Maclean, J., Oates, P., Shaw, G., Tanvir, N., Taylor, K., Taylor, P., Webster, J., & Worswick, S. 1994, PASP, 106, 983

Appenzeller, I., Fricke, K., Fürtig, W., Gässler, W., Häfner, R., Harke, R., Hess, H.-J., Hummel, W., Jürgens, P., Kudritzki, R.-P., Mantel, K.-H., Meisl, W., Muschielok, B., Nicklas, H., Rupprecht, G., Seifert, W., Stahl, O., Szeifert, T., & Tarantik, K. 1998, The Messenger, 94, 1

Astier, P., Guy, J., Regnault, N., Pain, R., Aubourg, E., Balam, D., Basa, S., Carlberg, R. G., Fabbro, S., Fouchez, D., Hook, I. M., Howell, D. A., Lafoux, H., Neill, J. D., Palanque-Delabrouille, N., Perrett, K., Pritchet, C. J., Rich, J., Sullivan, M., Taillet, R., Aldering, G., Antilogus, P., Arsenijevic, V., Balland, C., Baumont, S., Bronder, J., Courtois, H., Ellis, R. S., Filiol, M., Gonçalves, A. C., Goobar, A., Guide, D., Hardin, D., Lusset, V., Lidman, C., McMahon, R., Mouchet, M., Mourao, A., Perlmutter, S., Ripoche, P., Tao, C., & Walton, N. 2006, A&A, 447, 31

Balland, C., Mouchet, M., Amanullah, R., Astier, P., Fabbro, S., Folatelli, G., Garavini, G., Goobar, A., Hardin, D., Irwin, M. J., McMahon, R. G., Mourão, A.-M., Nobili, S., Pain, R., Pascoal, R., Raux, J., Sainton, G., Schahmaneche, K., & Walton, N. A. 2007, A&A, 464, 827

Barris, B. J. & Tonry, J. L. 2004, ApJ, 613, L21

Blondin, S., Davis, T. M., Krisciunas, K., Schmidt, B. P., Sollerman, J., Wood-Vasey, W. M., Becker, A. C., Challis, P., Clocchiatti, A., Damke, G., Filippenko, A. V., Foley, R. J., Garnavich, P. M., Jha, S. W., Kirshner, R. P., Leibundgut, B., Li, W., Matheson, T., Miknaitis, G., Narayan, G., Pignata, G., Rest, A., Riess, A. G., Silverman, J. M., Smith, R. C., Spyromilio, J., Stritzinger, M., Stubbs, C. W., Suntzeff, N. B., Tonry, J. L., Tucker, B. E., & Zenteno, A. 2008, ApJ, 682, 724

Blondin, S., Dessart, L., Leibundgut, B., Branch, D., Höflich, P., Tonry, J. L., Matheson, T., Foley, R. J., Chornock, R., Filippenko, A. V., Sollerman, J., Spyromilio, J., Kirshner, R. P., Wood-Vasey, W. M., Clocchiatti, A., Aguilera, C., Barris, B., Becker, A. C., Challis, P., Covarrubias, R., Davis, T. M., Garnavich, P., Hicken, M., Jha, S., Krisciunas, K., Li, W., Miceli, A., Miknaitis, G., Pignata, G., Prieto, J. L., Rest, A., Riess, A. G., Salvo, M. E., Schmidt, B. P., Smith, R. C., Stubbs, C. W., & Suntzeff, N. B. 2006, AJ, 131, 1648

Blondin, S. & Tonry, J. L. 2007, ApJ, 666, 1024

Blondin, S., Walsh, J. R., Leibundgut, B., & Sainton, G. 2005, A&A, 431, 757

Branch, D., Fisher, A., & Nugent, P. 1993, AJ, 106, 2383

Bronder, T. J., Hook, I. M., Astier, P., Balam, D., Balland, C., Basa, S., Carlberg, R. G., Conley, A., Fouchez, D., Guy, J., Howell, D. A., Neill, J. D., Pain, R., Perrett, K., Pritchet, C. J., Regnault, N., Sullivan, M., Baumont, S., Fabbro, S., Filliol, M., Perlmutter, S., & Ripoche, P. 2008, A&A, 477, 717

Davis, T. M., Mörtsell, E., Sollerman, J., Becker, A. C., Blondin, S., Challis, P., Clocchiatti, A., Filippenko, A. V., Foley, R. J., Garnavich, P. M., Jha, S., Krisciunas, K., Kirshner, R. P., Leibundgut, B., Li, W., Matheson, T., Miknaitis, G., Pignata, G., Rest, A., Riess, A. G., Schmidt, B. P., Smith, R. C., Spyromilio, J., Stubbs, C. W., Suntzeff, N. B., Tonry, J. L., Wood-Vasey, W. M., & Zenteno, A. 2007, ApJ, 666, 716

Dressler, A., Hare, T., Bigelow, B. C., & Osip, D. J. 2006, in Presented at the Society of Photo-Optical Instrumentation Engineers (SPIE) Conference, Vol. 6269, Ground-based and Airborne Instrumentation for Astronomy. Edited by McLean, Ian S.; Iye, Masanori. Proceedings of the SPIE, Volume 6269, pp. 62690F (2006).

Ellis, R. S., Sullivan, M., Nugent, P. E., Howell, D. A., Gal-Yam, A., Astier, P., Balam, D., Balland, C., Basa, S., Carlberg, R. G., Conley, A., Fouchez, D., Guy, J., Hardin, D., Hook, I., Pain, R., Perrett, K., Pritchet, C. J., & Regnault, N. 2008, ApJ, 674, 51

Faber, S. M., Phillips, A. C., Kibrick, R. I., Alcott, B., Allen, S. L., Burrous, J., Cantrall, T., Clarke, D., Coil, A. L., Cowley, D. J., Davis, M., Deich, W. T. S., Dietsch, K., Gilmore, D. K., Harper, C. A., Hilyard, D. F., Lewis, J. P., McVeigh, M., Newman, J., Osborne, J., Schiavon, R., Stover, R. J., Tucker, D., Wallace, V., Wei, M., Wirth, G., & Wright, C. A. 2003, in Instrument Design and Performance for Optical/Infrared Ground-based Telescopes. Edited by Iye, Masanori; Moorwood, Alan F. M. Proceedings of the SPIE, Volume 4841, pp. 1657-1669 (2003)., ed. M. Iye & A. F. M. Moorwood, 1657–1669

Fabricant, D., Cheimets, P., Caldwell, N., & Geary, J. 1998, PASP, 110, 79

Filippenko, A. V. 1988, AJ, 96, 1941

—. 1997, ARA&A, 35, 309

Filippenko, A. V. 2005, in Astrophysics and Space Science Library, Vol. 332, White dwarfs: cosmological and galactic probes, ed. E. M. Sion, S. Vennes, & H. L. Shipman (Dordrecht: Springer), 97–133

Filippenko, A. V., Matheson, T., & Ho, L. C. 1993, ApJ, 415, L103+

Filippenko, A. V., Richmond, M. W., Branch, D., Gaskell, M., Herbst, W., Ford, C. H., Treffers, R. R., Matheson, T., Ho, L. C., Dey, A., Sargent, W. L. W., Small, T. A., & van Breugel, W. J. M. 1992a, AJ, 104, 1543

Filippenko, A. V., Richmond, M. W., Matheson, T., Shields, J. C., Burbidge, E. M., Cohen, R. D., Dickinson, M., Malkan, M. A., Nelson, B., Pietz, J., Schlegel, D., Schmeer, P., Spinrad, H., Steidel, C. C., Tran, H. D., & Wren, W. 1992b, ApJ, 384, L15

Foley, R. J., Filippenko, A. V., Aguilera, C., Becker, A. C., Blondin, S., Challis, P., Clocchiatti, A., Covarrubias, R., Davis, T. M., Garnavich, P. M., Jha, S. W., Kirshner, R. P., Krisciunas, K., Leibundgut, B., Li, W., Matheson, T., Miceli, A., Miknaitis, G., Pignata, G., Rest, A., Riess, A. G., Schmidt, B. P., Smith, R. C., Sollerman, J., Spyromilio, J., Stubbs, C. W., Suntzeff, N. B., Tonry, J. L., Wood-Vasey, W. M., & Zenteno, A. 2008, ApJ, 684, 68

Foley, R. J., Papenkova, M. S., Swift, B. J., Filippenko, A. V., Li, W., Mazzali, P. A., Chornock, R., Leonard, D. C., & Van Dyk, S. D. 2003, PASP, 115, 1220

Galama, T. J., Vreeswijk, P. M., van Paradijs, J., Kouveliotou, C., Augusteijn, T., Böhnhardt, H., Brewer, J. P., Doublier, V., Gonzalez, J.-F., Leibundgut, B., Lidman, C., Hainaut, O. R., Patat, F., Heise, J., in't Zand, J., Hurley, K., Groot, P. J., Strom, R. G., Mazzali, P. A., Iwamoto, K., Nomoto, K., Umeda, H., Nakamura, T., Young, T. R., Suzuki, T., Shigeyama, T., Koshut, T., Kippen, M., Robinson, C., de Wildt, P., Wijers, R. A. M. J., Tanvir, N., Greiner, J., Pian, E., Palazzi, E., Frontera, F., Masetti, N., Nicastro, L., Feroci, M., Costa, E., Piro, L., Peterson, B. A., Tinney, C., Boyle, B., Cannon, R., Stathakis, R., Sadler, E., Begam, M. C., & Ianna, P. 1998, Nature, 395, 670

Garavini, G., Folatelli, G., Goobar, A., Nobili, S., Aldering, G., Amadon, A., Amanullah, R., Astier, P., Balland, C., Blanc, G., Burns, M. S., Conley, A., Dahlén, T., Deustua, S. E., Ellis, R., Fabbro, S., Fan, X., Frye, B., Gates, E. L., Gibbons, R., Goldhaber, G., Goldman, B., Groom, D. E., Haissinski, J., Hardin, D., Hook, I. M., Howell, D. A., Kasen, D., Kent, S., Kim, A. G., Knop, R. A., Lee, B. C., Lidman, C., Mendez, J., Miller, G. J., Moniez, M., Mourão, A., Newberg, H., Nugent, P. E., Pain, R., Perdereau, O., Perlmutter, S., Prasad, V., Quimby, R., Raux, J., Regnault, N., Rich, J., Richards, G. T., Ruiz-Lapuente, P., Sainton, G., Schaefer, B. E., Schahmaneche, K., Smith, E., Spadafora, A. L., Stanishev, V., Walton, N. A., Wang, L., & Wood-Vasey, W. M. 2004, AJ, 128, 387

Garavini, G., Folatelli, G., Nobili, S., Aldering, G., Amanullah, R., Antilogus, P., Astier, P., Blanc, G., Bronder, T., Burns, M. S., Conley, A., Deustua, S. E., Doi, M., Fabbro, S., Fadeyev, V., Gibbons, R., Goldhaber, G., Goobar, A., Groom, D. E., Hook, I., Howell, D. A., Kashikawa, N., Kim, A. G., Kowalski, M., Kuznetsova, N., Lee, B. C., Lidman, C., Mendez, J., Morokuma, T., Motohara, K., Nugent, P. E., Pain, R., Perlmutter, S., Quimby, R., Raux, J., Regnault, N., Ruiz-Lapuente, P., Sainton, G., Schahmaneche, K., Smith, E., Spadafora, A. L., Stanishev, V., Thomas, R. C., Walton, N. A., Wang, L., Wood-Vasey, W. M., & Yasuda, N. 2007, A&A, 470, 411

Glazebrook, K. & Bland-Hawthorn, J. 2001, PASP, 113, 197

Guy, J., Astier, P., Baumont, S., Hardin, D., Pain, R., Regnault, N., Basa, S., Carlberg, R. G., Conley, A., Fabbro, S., Fouchez, D., Hook, I. M., Howell, D. A., Perrett, K., Pritchet, C. J., Rich, J., Sullivan, M., Antilogus, P., Aubourg, E., Bazin, G., Bronder, J., Filiol, M., Palanque-Delabrouille, N., Ripoche, P., & Ruhlmann-Kleider, V. 2007, A&A, 466, 11

Hook, I. M., Jørgensen, I., Allington-Smith, J. R., Davies, R. L., Metcalfe, N., Murowinski, R. G., & Crampton, D. 2004, PASP, 116, 425

Horne, K. 1986, PASP, 98, 609

Howell, D. A., Sullivan, M., Perrett, K., Bronder, T. J., Hook, I. M., Astier, P., Aubourg, E., Balam, D., Basa, S., Carlberg, R. G., Fabbro, S., Fouchez, D., Guy, J., Lafoux, H., Neill, J. D., Pain, R., Palanque-Delabrouille, N., Pritchet, C. J., Regnault, N., Rich, J., Taillet, R., Knop, R., McMahon, R. G., Perlmutter, S., & Walton, N. A. 2005, ApJ, 634, 1190

Jha, S., Riess, A. G., & Kirshner, R. P. 2007, ApJ, 659, 122

Kowalski, M., Rubin, D., Aldering, G., Agostinho, R. J., Amadon, A., Amanullah, R., Balland, C., Barbary, K., Blanc, G., Challis, P. J., Conley, A., Connolly, N. V., Covarrubias, R., Dawson, K. S., Deustua, S. E., Ellis, R., Fabbro, S., Fadeyev, V., Fan, X., Farris, B., Folatelli, G., Frye, B. L., Garavini, G., Gates, E. L., Germany, L., Goldhaber, G., Goldman, B., Goobar, A., Groom, D. E., Haissinski, J., Hardin, D., Hook, I., Kent, S., Kim, A. G., Knop, R. A., Lidman, C., Linder, E. V., Mendez, J., Meyers, J., Miller, G. J., Moniez, M., Mourão, A. M., Newberg, H., Nobili, S., Nugent, P. E., Pain, R., Perdereau, O., Perlmutter, S., Phillips, M. M., Prasad, V., Quimby, R., Regnault, N., Rich, J., Rubenstein, E. P., Ruiz-Lapuente, P., Santos, F. D., Schaefer, B. E., Schommer, R. A., Smith, R. C., Soderberg, A. M., Spadafora, A. L., Strolger, L.-G., Strovink, M., Suntzeff, N. B., Suzuki, N., Thomas, R. C., Walton, N. A., Wang, L., Wood-Vasey, W. M., & Yun, J. L. 2008, ApJ, 686, 749

Leibundgut, B., Kirshner, R. P., Phillips, M. M., Wells, L. A., Suntzeff, N. B., Hamuy, M., Schommer, R. A., Walker, A. R., Gonzalez, L., Ugarte, P., Williams, R. E., Williger, G., Gomez, M., Marzke, R., Schmidt, B. P., Whitney, B., Coldwell, N., Peters, J., Chaffee, F. H., Foltz, C. B., Rehner, D., Siciliano, L., Barnes, T. G., Cheng, K.-P., Hintzen, P. M., Kim, Y.-C., Maza, J., Parker, J. W., Porter, A. C., Schmidtke, P. C., & Sonneborn, G. 1993, AJ, 105, 301

Li, W., Filippenko, A. V., Chornock, R., Berger, E., Berlind, P., Calkins, M. L., Challis, P., Fassnacht, C., Jha, S., Kirshner, R. P., Matheson, T., Sargent, W. L. W., Simcoe, R. A., Smith, G. H., & Squires, G. 2003, PASP, 115, 453

Li, W., Filippenko, A. V., Gates, E., Chornock, R., Gal-Yam, A., Ofek, E. O., Leonard, D. C., Modjaz, M., Rich, R. M., Riess, A. G., & Treffers, R. R. 2001a, PASP, 113, 1178

Li, W., Filippenko, A. V., Treffers, R. R., Riess, A. G., Hu, J., & Qiu, Y. 2001b, ApJ, 546, 734

Matheson, T., Blondin, S., Foley, R. J., Chornock, R., Filippenko, A. V., Leibundgut, B., Smith, R. C., Sollerman, J., Spyromilio, J., Kirshner, R. P., Clocchiatti, A., Aguilera, C., Barris, B., Becker, A. C., Challis, P., Covarrubias, R., Garnavich, P., Hicken, M., Jha, S., Krisciunas, K., Li, W., Miceli, A., Miknaitis, G., Prieto, J. L., Rest, A., Riess, A. G., Salvo, M. E., Schmidt, B. P., Stubbs, C. W., Suntzeff, N. B., & Tonry, J. L. 2005, AJ, 129, 2352

Matheson, T., Filippenko, A. V., Ho, L. C., Barth, A. J., & Leonard, D. C. 2000, AJ, 120, 1499

Matheson, T., Kirshner, R. P., Challis, P., Jha, S., Garnavich, P. M., Berlind, P., Calkins, M. L., Blondin, S., Balog, Z., Bragg, A. E., Caldwell, N., Dendy Concannon, K., Falco, E. E., Graves, G. J. M., Huchra, J. P., Kuraszkiewicz, J., Mader, J. A., Mahdavi, A., Phelps, M., Rines, K., Song, I., & Wilkes, B. J. 2008, AJ, 135, 1598

Miknaitis, G., Pignata, G., Rest, A., Wood-Vasey, W. M., Blondin, S., Challis, P., Smith, R. C., Stubbs, C. W., Suntzeff, N. B., Foley, R. J., Matheson, T., Tonry, J. L., Aguilera, C., Blackman, J. W., Becker, A. C., Clocchiatti, A., Covarrubias, R., Davis, T. M., Filippenko, A. V., Garg, A., Garnavich, P. M., Hicken, M., Jha, S., Krisciunas, K., Kirshner, R. P., Leibundgut, B., Li, W., Miceli, A., Narayan, G., Prieto, J. L., Riess, A. G., Salvo, M. E., Schmidt, B. P., Sollerman, J., Spyromilio, J., & Zenteno, A. 2007, ApJ, 666, 674

Oke, J. B., Cohen, J. G., Carr, M., Cromer, J., Dingizian, A., Harris, F. H., Labrecque, S., Lucinio, R., Schaal, W., Epps, H., & Miller, J. 1995, PASP, 107, 375

Perlmutter, S., Aldering, G., Goldhaber, G., Knop, R. A., Nugent, P., Castro, P. G., Deustua, S., Fabbro, S., Goobar, A., Groom, D. E., Hook, I. M., Kim, A. G., Kim, M. Y., Lee, J. C., Nunes, N. J., Pain, R., Pennypacker, C. R., Quimby, R., Lidman, C., Ellis, R. S., Irwin, M., McMahon, R. G., Ruiz-Lapuente, P., Walton, N., Schaefer, B., Boyle, B. J., Filippenko, A. V., Matheson, T., Fruchter, A. S., Panagia, N., Newberg, H. J. M., & Couch, W. J. 1999, ApJ, 517, 565

Phillips, M. M. 1993, ApJ, 413, L105

Phillips, M. M., Wells, L. A., Suntzeff, N. B., Hamuy, M., Leibundgut, B., Kirshner, R. P., & Foltz, C. B. 1992, AJ, 103, 1632

Poznanski, D., Maoz, D., Yasuda, N., Foley, R. J., Doi, M., Filippenko, A. V., Fukugita, M., Gal-Yam, A., Jannuzi, B. T., Morokuma, T., Oda, T., Schweiker, H., Sharon, K., Silverman, J. M., & Totani, T. 2007, MNRAS, 382, 1169

Riess, A. G., Filippenko, A. V., Challis, P., Clocchiatti, A., Diercks, A., Garnavich, P. M., Gilliland, R. L., Hogan, C. J., Jha, S., Kirshner, R. P., Leibundgut, B., Phillips, M. M., Reiss, D., Schmidt, B. P., Schommer, R. A., Smith, R. C., Spyromilio, J., Stubbs, C., Suntzeff, N. B., & Tonry, J. 1998, AJ, 116, 1009

Riess, A. G., Press, W. H., & Kirshner, R. P. 1996, ApJ, 473, 88

Riess, A. G., Strolger, L.-G., Casertano, S., Ferguson, H. C., Mobasher, B., Gold, B., Challis, P. J., Filippenko, A. V., Jha, S., Li, W., Tonry, J., Foley, R., Kirshner, R. P., Dickinson, M., MacDonald, E., Eisenstein, D., Livio, M., Younger, J., Xu, C., Dahlén, T., & Stern, D. 2007, ApJ, 659, 98

Schmidt, G. D., Weymann, R. J., & Foltz, C. B. 1989, PASP, 101, 713

Strolger, L.-G., Smith, R. C., Suntzeff, N. B., Phillips, M. M., Aldering, G., Nugent, P., Knop, R., Perlmutter, S., Schommer, R. A., Ho, L. C., Hamuy, M., Krisciunas, K., Germany, L. M., Covarrubias, R., Candia, P., Athey, A., Blanc, G., Bonacic, A., Bowers, T., Conley, A., Dahlén, T., Freedman, W., Galaz, G., Gates, E., Goldhaber, G., Goobar, A., Groom, D., Hook, I. M., Marzke, R., Mateo, M., McCarthy, P., Méndez, J., Muena, C., Persson, S. E., Quimby, R., Roth, M., Ruiz-Lapuente, P., Seguel, J., Szentgyorgyi, A., von Braun, K., Wood-Vasey, W. M., & York, T. 2002, AJ, 124, 2905

Tonry, J. L., Schmidt, B. P., Barris, B., Candia, P., Challis, P., Clocchiatti, A., Coil, A. L., Filippenko, A. V., Garnavich, P., Hogan, C., Holland, S. T., Jha, S., Kirshner, R. P., Krisciunas, K., Leibundgut, B., Li, W., Matheson, T., Phillips, M. M., Riess, A. G., Schommer, R., Smith, R. C., Sollerman, J., Spyromilio, J., Stubbs, C. W., & Suntzeff, N. B. 2003, ApJ, 594, 1

Turatto, M. 2003, in Lecture Notes in Physics, Berlin Springer Verlag, Vol. 598, Supernovae and Gamma-Ray Bursters, ed. K. Weiler, 21–36

Wade, R. A. & Horne, K. 1988, ApJ, 324, 411

Wood-Vasey, W. M., Miknaitis, G., Stubbs, C. W., Jha, S., Riess, A. G., Garnavich, P. M., Kirshner, R. P., Aguilera, C., Becker, A. C., Blackman, J. W., Blondin, S., Challis, P., Clocchiatti, A., Conley, A., Covarrubias, R., Davis, T. M., Filippenko, A. V., Foley, R. J., Garg, A., Hicken, M., Krisciunas, K., Leibundgut, B., Li, W., Matheson, T., Miceli, A., Narayan, G., Pignata, G., Prieto, J. L., Rest, A., Salvo, M. E., Schmidt, B. P., Smith, R. C., Sollerman, J., Spyromilio, J., Tonry, J. L., Suntzeff, N. B., & Zenteno, A. 2007, ApJ, 666, 694

TABLE 2
ESSENCE SPECTROSCOPIC TARGETS

ESSENCE ID[a]	IAUC ID[b]	UT Date	Telescope	Type[c]	Subtype	z (Gal)[d]	z (SNID)[e]	Template	Phase (SNID) (d)	Phase (LC) (d)	Δ	Disc. Mag.	Exp. (s)
a002.wxc1_04	$\cdots$	2002-12-06.03	VLT	Gal	$\cdots$	0.315	$\cdots$	$\cdots$	$\cdots$	$\cdots$	$\cdots$	$\cdots$	900
b001.wxc1_14	$\cdots$	2002-11-03.23	MMT	Unk	$\cdots$	$\cdots$	$\cdots$	$\cdots$	$\cdots$	$\cdots$	$\cdots$	$\cdots$	1800
b001.wxc1_14	$\cdots$	2002-11-06.27	KII/ESI	Unk	$\cdots$	$\cdots$	$\cdots$	$\cdots$	$\cdots$	$\cdots$	$\cdots$	$\cdots$	1600
b001.wxc1_14	$\cdots$	2002-11-11.32	KI/LRIS	Unk	$\cdots$	$\cdots$	$\cdots$	$\cdots$	$\cdots$	$\cdots$	$\cdots$	$\cdots$	1800
b001.wxc1_14	$\cdots$	2002-12-05.26	GMOS	Unk	$\cdots$	$\cdots$	$\cdots$	$\cdots$	$\cdots$	$\cdots$	$\cdots$	$\cdots$	2x1800
b002.wxh1_01	$\cdots$	2002-11-01.44	KII/ESI	Star	$\cdots$	$\cdots$	$\cdots$	$\cdots$	$\cdots$	$\cdots$	$\cdots$	$\cdots$	900
b003.wxh1_14	2002iu	2002-11-01.43	KII/ESI	Ia	norm	$\cdots$	0.115 (0.005)	1999ee	-3.8 (3.2)	$\cdots$	$\cdots$	$\cdots$	600
b004.wxt2_06	2002iv	2002-11-02.45	KII/ESI	Ia	91T	0.231	0.226 (0.006)	2005eq	-4.9 (1.6)	$\cdots$	$\cdots$	$\cdots$	1200
b005.wxd1_11	2002iw	2002-11-03.16	MMT	Gal	$\cdots$	0.205	$\cdots$	$\cdots$	$\cdots$	$\cdots$	$\cdots$	$\cdots$	3x1800
b005.wxd1_11	2002iw	2002-11-06.32	KII/ESI	Gal	$\cdots$	0.205	$\cdots$	$\cdots$	$\cdots$	$\cdots$	$\cdots$	$\cdots$	1800
b006.wxb1_16	2002ix	2002-11-03.10	MMT	N.S.	$\cdots$	$\cdots$	$\cdots$	$\cdots$	$\cdots$	$\cdots$	$\cdots$	21.7	$\cdots$
b006.wxb1_16	2002ix	2002-11-06.24	KII/ESI	II?	$\cdots$	$\cdots$	$\cdots$	$\cdots$	$\cdots$	$\cdots$	$\cdots$	21.7	1800
b008.wxc1_05	2002jq	2002-11-06.29	KII/ESI	Ia	$\cdots$	$\cdots$	$\cdots$	$\cdots$	$\cdots$	$\cdots$	$\cdots$	$\cdots$	1800
b008.wxc1_05	2002jq	2002-12-04.27	GMOS	Ia	norm	$\cdots$	0.473 (0.003)	1990N	14.5 (2.4)	$\cdots$	$\cdots$	$\cdots$	4x1800
b010.wxv2_07	2002iy	2002-11-06.39	KII/ESI	Ia	$\cdots$	$\cdots$	0.587 (0.006)	2000cx	-4.2 (1.6)	-7.8 (1.7)	-0.166	23.0	1800
b010.wxv2_07	2002iy	2002-11-11.45	KI/LRIS	Ia	$\cdots$	$\cdots$	$\cdots$	$\cdots$	$\cdots$	-2.8 (1.7)	-0.166	23.0	1800
b010.wxv2_07	2002iy	2002-12-06.35	GMOS	Ia	norm	$\cdots$	0.587 (0.007)	1999ee	11.1 (5.4)	22.2 (1.7)	-0.166	23.0	5x1800
b010.wxv2_07	2002iy	2002-12-07.22	VLT	Ia	norm	$\cdots$	0.587 (0.007)	1999ee	11.1 (5.4)	23.2 (1.7)	-0.166	23.0	2x1800
b013.wxv2_10	2002iz	2002-11-06.45	KII/ESI	Ia	norm	0.427	0.425 (0.005)	1994D	-2.0 (1.5)	-1.3 (1.1)	0.034	22.2	1800
b013.wxv2_10	2002iz	2002-12-06.07	VLT	Ia	norm	0.427	0.428 (0.004)	1995D	17.0 (1.8)	28.7 (1.1)	0.034	22.2	1800+71
b014.wxv2_15	$\cdots$	2002-11-06.41	KII/ESI	Gal	$\cdots$	0.268	$\cdots$	$\cdots$	$\cdots$	$\cdots$	$\cdots$	22.5	1800
b015.wcx1_09	$\cdots$	2002-11-06.34	KII/ESI	Gal	$\cdots$	0.207	$\cdots$	$\cdots$	$\cdots$	$\cdots$	$\cdots$	$\cdots$	1800
b016.wxb1_15	2002ja	2002-11-09.33	KII/ESI	Ia	norm	$\cdots$	0.325 (0.002)	2005hj	2.5 (4.9)	0.2 (1.7)	0.190	22.2	1200
b017.wxb1_06	2002jb	2002-11-09.31	KII/ESI	Ia	norm	$\cdots$	0.260 (0.006)	2002bo	-2.5 (2.9)	$\cdots$	$\cdots$	21.4	1200
b019.wxd1_04	$\cdots$	2002-11-09.35	KII/ESI	Gal	$\cdots$	0.213	$\cdots$	$\cdots$	$\cdots$	$\cdots$	$\cdots$	$\cdots$	1200
b020.wye2_01	2002jr	2002-11-09.42	KII/ESI	Ia	norm	$\cdots$	0.424 (0.004)	2004dt	-4.6 (2.7)	-11.9 (0.6)	0.059	22.2	1800
b020.wye2_01	2002jr	2002-12-09.39	GMOS	Ia	$\cdots$	$\cdots$	0.428 (0.004)	2001eh	8.9 (1.1)	18.1 (0.6)	0.059	22.2	2x1800
b022.wyc3_03	2002jc	2002-11-09.45	KII/ESI	Ia	$\cdots$	$\cdots$	$\cdots$	$\cdots$	$\cdots$	$\cdots$	$\cdots$	22.4	1800
b022.wyc3_03	2002jc	2002-12-05.39	GMOS	Ia	norm	$\cdots$	0.528 (0.005)	1995E	6.9 (1.8)	$\cdots$	$\cdots$	22.4	4x1800
b023.wxu2_09	2002js	2002-11-11.57	KI/LRIS	Ia	$\cdots$	$\cdots$	$\cdots$	$\cdots$	$\cdots$	$\cdots$	$\cdots$	$\cdots$	2100
b023.wxu2_09	2002js	2002-12-03.41	GMOS	Ia	norm	$\cdots$	0.541 (0.005)	2004eo	5.5 (2.2)	$\cdots$	$\cdots$	$\cdots$	4x1800
b024.wxc1_16	$\cdots$	2002-11-11.27	KI/LRIS	Star	$\cdots$	0.000	$\cdots$	$\cdots$	$\cdots$	$\cdots$	$\cdots$	$\cdots$	1800
b025.wxa1_05	$\cdots$	2002-11-11.29	KI/LRIS	N.S.	$\cdots$	$\cdots$	$\cdots$	$\cdots$	$\cdots$	$\cdots$	$\cdots$	$\cdots$	1800
b026.wxk1_05	$\cdots$	2002-11-11	KI/LRIS	N.S.	$\cdots$	$\cdots$	$\cdots$	$\cdots$	$\cdots$	$\cdots$	$\cdots$	$\cdots$	$\cdots$
b027.wxm1_16	2002jd	2002-11-11.45	KI/LRIS	Ia	norm	$\cdots$	0.315 (0.007)	2006ax	-3.5 (4.7)	$\cdots$	$\cdots$	$\cdots$	3600,1800[k]
b027.wxm1_16	2002jd	2002-12-08.07	VLT	Ia	$\cdots$	$\cdots$	$\cdots$	$\cdots$	$\cdots$	$\cdots$	$\cdots$	$\cdots$	1091
b027.wxm1_16	2002jd	2002-12-09.27	GMOS	Ia	$\cdots$	$\cdots$	$\cdots$	$\cdots$	$\cdots$	$\cdots$	$\cdots$	$\cdots$	4x1800
c002.wxp1_14	$\cdots$	2002-12-01	Clay	N.S.	$\cdots$	$\cdots$	$\cdots$	$\cdots$	$\cdots$	$\cdots$	$\cdots$	$\cdots$	$\cdots$
c002.wxp1_14	$\cdots$	2002-12-03	GMOS	N.S.	$\cdots$	$\cdots$	$\cdots$	$\cdots$	$\cdots$	$\cdots$	$\cdots$	$\cdots$	$\cdots$
c003.wxh1_15	2002jt	2002-12-02.13	Clay	Ia	$\cdots$	$\cdots$	0.570 (0.007)	2001eh	1.0 (3.5)	$\cdots$	$\cdots$	$\cdots$	2x1800
c003.wxh1_15	2002jt	2002-12-07.29	GMOS	Ia	$\cdots$	$\cdots$	$\cdots$	$\cdots$	$\cdots$	$\cdots$	$\cdots$	$\cdots$	3x1800
c005.wxb1_10	$\cdots$	2002-12-06.05	VLT	AGN	$\cdots$	0.249	$\cdots$	$\cdots$	$\cdots$	$\cdots$	$\cdots$	$\cdots$	900
c012.wxu2_16[l]	2002ju	2002-12-03.15	Clay	Ia	$\cdots$	0.348	0.349 (0.005)	2000E	-2.5 (2.7)	$\cdots$	$\cdots$	$\cdots$	2x1800
c012.wxu2_16[l]	2002ju	2002-12-04.43	GMOS	Ia	$\cdots$	0.348	0.349 (0.005)	2000E	-2.5 (2.7)	$\cdots$	$\cdots$	$\cdots$	3x1200
c012.wxu2_16	2002ju	2003-01-05.33	KII/ESI	Ia	$\cdots$	0.348	$\cdots$	$\cdots$	$\cdots$	$\cdots$	$\cdots$	$\cdots$	1800
c013.wxm1_13	$\cdots$	2002-12-05	GMOS	N.S.	$\cdots$	$\cdots$	$\cdots$	$\cdots$	$\cdots$	$\cdots$	$\cdots$	$\cdots$	$\cdots$
c014.wyb3_03	2002jv	2002-12-07.12	VLT	Gal	$\cdots$	0.221	$\cdots$	$\cdots$	$\cdots$	$\cdots$	$\cdots$	22.4	2x1800
c014.wyb3_03	2002jv	2003-01-04.28	GMOS	Gal	$\cdots$	0.221	$\cdots$	$\cdots$	$\cdots$	$\cdots$	$\cdots$	22.4	4x1800
c015.wxv2_02	2002jw	2002-12-07.18	VLT	Ia	norm	0.357	0.356 (0.007)	2003du	-2.8 (2.8)	$\cdots$	$\cdots$	22.7	2x1800
c015.wxv2_02	2002jw	2003-01-05.37	KII/ESI	Ia	$\cdots$	0.357	$\cdots$	$\cdots$	$\cdots$	$\cdots$	$\cdots$	22.7	2400
c016.wxm1_04	$\cdots$	2002-12-07.07	VLT	Gal	$\cdots$	0.845	$\cdots$	$\cdots$	$\cdots$	$\cdots$	$\cdots$	$\cdots$	2x1800
c020.wxt2_15	$\cdots$	2003-01-05.30	KII/ESI	Unk	$\cdots$	$\cdots$	$\cdots$	$\cdots$	$\cdots$	$\cdots$	$\cdots$	$\cdots$	2x900
c020.wxt2_15	$\cdots$	2003-01-10.11	VLT	Unk	$\cdots$	$\cdots$	$\cdots$	$\cdots$	$\cdots$	$\cdots$	$\cdots$	$\cdots$	2x1800

TABLE 2 — *Continued*

ESSENCE ID[a]	IAUC ID[b]	UT Date	Telescope	Type[c]	Subtype	z (Gal)[d]	z (SNID)[e]	Template	Phase (SNID) (d)	Phase (LC) (d)	Δ	Disc. Mag.	Exp. (s)
c022.wxu2_15	⋯	2003-01-04.09	Clay	Ib	IIb	0.213	0.211 (0.004)	1997dd	7.4 (13.8)	⋯	⋯	⋯	2x1200
c023.wxm1_15	⋯	2003-01-03.07	Clay	Ia	norm	0.399	0.412 (0.001)	1999ee	⋯	⋯	⋯	⋯	2x1200
c024.wxv2_05	⋯	2003-01-03.12	Clay	Gal	⋯	0.317	⋯	⋯	⋯	⋯	⋯	22.8	1800
c025.wxb1_14	⋯	2003-01-04.05	Clay	AGN	⋯	0.362	⋯	⋯	⋯	⋯	⋯	19.7	600
c028.wxu2_16	⋯	2003-01-04.13	Clay	AGN	⋯	2.020	⋯	⋯	⋯	⋯	⋯	⋯	1800
d009.waa6_16[m]	⋯	2003-10-29.11	VLT	Ia	91T	0.354	0.351 (0.002)	1998ab	22.7 (14.5)	⋯	⋯	⋯	1800
d106.waa6_16[m]	⋯	2003-10-31.01	VLT	Ia	⋯	0.353	⋯	⋯	⋯	⋯	⋯	⋯	1800
d010.waa6_16	2003jp	2003-10-30.03	VLT	Ic	norm	0.083	0.080 (0.001)	1991A	⋯	⋯	⋯	⋯	2x1800
d029.waa6_13	⋯	2003-10-29.03	VLT	AGN	⋯	2.583	⋯	⋯	⋯	⋯	⋯	⋯	2x1800
d033.waa6_10	2003jo	2003-10-29.09	VLT	Ia	norm	0.526	0.530 (0.007)	2002er	2.0 (2.8)	7.7 (1.2)	−0.322	23.1	2x1800
d033.waa6_10	2003jo	2003-11-23.05	VLT	Ia	norm	0.526	0.530 (0.007)	2002er	2.0 (2.8)	32.7 (1.2)	−0.322	23.1	1800+900
d034.waa7_10	⋯	2003-10-28.29	GMOS	AGN	⋯	2.280	⋯	⋯	⋯	⋯	⋯	⋯	2x1200
d051.wcc8_2	⋯	2003-10-30.22	VLT	Gal	⋯	0.382	⋯	⋯	⋯	⋯	⋯	⋯	1800
d057.wbb6_3	2003jk	2003-10-30.15	VLT	Unk	⋯	⋯	⋯	⋯	⋯	⋯	⋯	22.2	2x1800
d058.wbb6_3	2003jj	2003-10-31.07	VLT	Ia	norm	0.584	0.589 (0.009)	1981B	−0.9 (2.3)	2.2	−0.470	22.8	2x1800
d059.wcc5_3	⋯	2003-10-29.17	VLT	Gal	⋯	0.207	⋯	⋯	⋯	⋯	⋯	22.5	2x1800
d060.wcc7_3	⋯	2003-10-30.35	VLT	Star	⋯	⋯	⋯	⋯	⋯	⋯	⋯	⋯	1800
d062.wcc9_3	⋯	2003-10-29.26	VLT	AGN	⋯	2.432	⋯	⋯	⋯	⋯	⋯	⋯	1800+368
d083.wdd9_12	2003jn	2003-10-29.29	VLT	Ia	91T	⋯	0.333 (0.001)	1998ab	−6.4 (1.9)	5.3 (0.6)	−0.273	20.7	1800
d084.wdd9_11	2003jm	2003-10-30.19	VLT	Ia	norm	0.522	0.516 (0.006)	1996X	3.6 (2.8)	5.8 (1.2)	−0.197	22.9	1800
d085.waa5_16	2003jv	2003-10-28.37	GMOS	Ia	⋯	0.405	0.401 (0.008)	2005hj	1.0 (2.5)	0.5 (0.6)	−0.228	22.0	3x1200
d086.waa5_3	2003ju	2003-10-27.06	GMOS	Ia	norm	⋯	0.211 (0.001)	1990N	⋯	−5.4 (0.3)	−0.177	21.0	3x600
d086.waa5_3	2003ju	2003-11-27.10	Baade	Ia	⋯	⋯	0.203 (0.003)	1999aw	19.5 (4.3)	25.6 (0.3)	−0.177	21.0	3x1800
d087.wbb5_4	2003jr	2003-11-01.18	GMOS	Ia	norm	0.340	0.337 (0.004)	1994D	15.1 (2.4)	20.0 (1.7)	−0.112	21.6	3x600
d089.wdd6_8	2003jl	2003-10-31.34	VLT	Ia	norm	⋯	0.425 (0.004)	1994ae	10.1 (1.0)	14.8 (1.5)	−0.198	22.0	1800
d091.wcc1_2	⋯	2003-10-29.22	VLT	Unk	⋯	⋯	⋯	⋯	⋯	⋯	⋯	23.6	2x1800
d093.wdd5_3[o]	2003js	2003-10-29.96	VLT	Ia	91T	0.363	0.359 (0.004)	1998es	−5.1 (1.7)	−4.3 (0.3)	−0.365	21.6	923+600
e142.wdd5_3[o]	2003js	2003-11-23.21	VLT	Ia	⋯	0.363	0.368 (0.005)	1995D	+12	⋯	⋯	21.6	3x1200
d097.wdd5_10	2003jt	2003-10-29.32	VLT	Ia	⋯	⋯	0.434 (0.007)	2001eh	3.1 (1.7)	6.6	−0.317	21.9	1800
d099.wcc2_16	2003ji	2003-11-01.23	GMOS	Ia	norm	⋯	0.210 (0.002)	2000fa	18.3 (1.8)	22.9 (1.6)	−0.110	21.0	3x600
d100.waa7_16	2003jq	2003-10-24.21	FLWO	Ia	norm	⋯	0.158 (0.003)	1994D	24.7 (9.9)	⋯	⋯	19.6	2x1800
d115.wbb6_11	⋯	2003-10-28.43	GMOS	Unk	⋯	⋯	⋯	⋯	⋯	⋯	⋯	21.8	1200
d117.wdd8_16	2003jw	2003-10-30.32	VLT	Ia	norm	0.297	0.301 (0.005)	2002bo	−4.5 (2.8)	−5.9 (0.4)	0.298	22.1	1800
d120.wcc1_2	⋯	2003-10-31.48	VLT	AGN	⋯	1.280	⋯	⋯	⋯	⋯	⋯	⋯	1800
d123.wcc9_16	⋯	2003-10-30.27	VLT	Gal	⋯	0.500	⋯	⋯	⋯	⋯	⋯	⋯	2x1800
d124.wcc9_15	⋯	2003-10-31.26	VLT	AGN	⋯	0.609	⋯	⋯	⋯	⋯	⋯	⋯	1800+1341
d149.wcc4_11	2003jy	2003-10-31.10	VLT	Ia	norm	0.339	0.338 (0.008)	1990O	−7.0 (1.8)	−10.5 (0.3)	−0.214	21.9	1800
d150.wcc1_12	⋯	2003-10-31.31	VLT	Gal	⋯	0.191	⋯	⋯	⋯	⋯	⋯	⋯	1800
d156.wcc2_4	2003jx	2003-10-31.15	VLT	Unk	⋯	⋯	⋯	⋯	⋯	⋯	⋯	⋯	2x1800
e018.wbb7_2	⋯	2003-11-19.05	Clay	AGN	⋯	0.181	⋯	⋯	⋯	⋯	⋯	> 24	600
e020.waa6_9	2003kk	2003-11-19.11	Clay	Ia	norm	0.164	0.159 (0.006)	2002er	−2.5 (3.8)	−2.3 (0.4)	−0.034	24.0	3x300
e022.wbb7_12	2003kj	2003-11-22.03	VLT	II	IIP	0.078	0.078 (0.004)	2005cs	4.0 (1.2)	⋯	⋯	> 24	1800+900
e025.wdd3_15	⋯	2003-11-19.21	Clay	Gal	⋯	0.180	⋯	⋯	⋯	⋯	⋯	22.6	3x1200
e027.wcc7_16	⋯	2003-11-21.16	VLT	Unk	⋯	⋯	⋯	⋯	⋯	⋯	⋯	23.5	3x1200
e029.wbb3_15[P]	2003kl	2003-11-19.14	Clay	Ia	norm	0.335	0.332 (0.007)	1990N	−4.4 (4.6)	−1.9 (0.7)	0.219	22.0	3x600
e121.wbb3_15[P]	2003kl	2003-11-22.11	Clay	Ia	⋯	0.335	0.326 (0.006)	1981B	−1	⋯	⋯	22.0	3x1200
e103.wbb9_2	⋯	2003-11-21.05	VLT	Unk	⋯	⋯	⋯	⋯	⋯	⋯	⋯	> 24	2x1800
e106.wbb6_11	⋯	2003-11-20.14	Clay	Unk	⋯	0.321	⋯	⋯	⋯	⋯	⋯	21.8	3x1200
e108.wdd8_4	2003km	2003-11-21.21	VLT	Ia	norm	⋯	0.472 (0.007)	1990O	−6.7 (2.7)	−14.6 (0.4)	−0.280	22.2	2x1800
e118.waa5_11	⋯	2003-11-22.03	VLT	AGN	⋯	0.557	⋯	⋯	⋯	⋯	⋯	21.7	2x1200
e119.wbb1_7	⋯	2003-11-23.19	VLT	Gal	⋯	0.558	⋯	⋯	⋯	⋯	⋯	22.5	1800+600
e120.waa5_9	⋯	2003-11-22.05	Clay	Gal	⋯	0.298	⋯	⋯	⋯	⋯	⋯	23.2	1200
e132.wcc1_7	2003kn	2003-11-22.08	VLT	Ia	norm	0.244	0.234 (0.006)	2003du	−6.4 (1.6)	−6.6 (0.3)	−0.128	21.4	2x1800
e133.wcc1_7	⋯	2003-11-22.08	VLT	Gal	⋯	0.244	⋯	⋯	⋯	⋯	⋯	22.6	2x1800
e136.wcc1_12	2003ko	2003-11-22.13	VLT	Ia	norm	0.361	0.346 (0.007)	2000cf	3.1 (4.1)	−1.3 (0.5)	0.332	22.1	2x1800

Foley et al.

TABLE 2 — *Continued*

ESSENCE ID[a]	IAUC ID[b]	UT Date	Telescope	Type[c]	Subtype	z (Gal)[d]	z (SNID)[e]	Template	Phase (SNID) (d)	Phase (LC) (d)	Δ	Disc. Mag.	Exp. (s)
e138.wdd4_1	2003kt	2003-11-23.10	VLT	Ia	norm	$\cdots$	0.611 (0.006)	1995D	5.3 (0.8)	10.8 (0.6)	-0.284	23.2	3x1200
e140.wdd5_15	2003kq	2003-11-22.29	VLT	Ia	norm	0.606	0.614 (0.006)	2006ax	-3.2 (2.8)	-2.1	-0.187	22.7	3x1200
e141.wdd7_2	$\cdots$	2003-11-22.16	Clay	Ib	IIb	0.099	0.084 (0.001)	1996cb	6.0 (5.4)	$\cdots$	$\cdots$	21.0	2x1200
e143.wdd7_3	$\cdots$	2003-11-23.15	VLT	Unk	$\cdots$	0.110	$\cdots$	$\cdots$	$\cdots$	$\cdots$	$\cdots$	22.0	2x1200
e147.wdd5_9	2003kp	2003-11-22.18	VLT	Ia	norm	$\cdots$	0.641 (0.008)	2003du	-1.1 (3.1)	2.0 (1.2)	-0.174	22.7	2x1800
e148.wdd5_10	2003kr	2003-11-22.23	VLT	Ia	norm	$\cdots$	0.429 (0.006)	1999ee	-6.7 (1.7)	-9.9 (0.4)	-0.107	22.1	3x1200
e149.wdd5_10	2003ks	2003-11-23.28	VLT	Ia	norm	$\cdots$	0.491 (0.006)	2006lf	11.5 (4.3)	16.2 (0.4)	0.016	22.5	3x1200
e309.waa9_14	$\cdots$	2003-11-23.32	GMOS	Star	$\cdots$	$\cdots$	$\cdots$	$\cdots$	$\cdots$	$\cdots$	$\cdots$	22.6	3x1200
e315.wbb9_3	2003ku	2003-11-24.31	GMOS	Ia?	$\cdots$	$\cdots$	0.81 (0.01)	$\cdots$	$\cdots$	$\cdots$	$\cdots$	> 24	3x1200
e418.wcc2_8	$\cdots$	2003-11-27	Baade	N.S.	$\cdots$	$\cdots$	$\cdots$	$\cdots$	$\cdots$	$\cdots$	$\cdots$	23.0	$\cdots$
e501.waa1_1	$\cdots$	2003-11-28	Baade	N.S.	$\cdots$	$\cdots$	$\cdots$	$\cdots$	$\cdots$	$\cdots$	$\cdots$	23.2	$\cdots$
e504.waa3_4	$\cdots$	2003-11-29.05	Baade	AGN	$\cdots$	0.674	$\cdots$	$\cdots$	$\cdots$	$\cdots$	$\cdots$	23.6	3x1800
e510.waa1_13	$\cdots$	2003-11-29.08	GMOS	Unk	$\cdots$	$\cdots$	$\cdots$	$\cdots$	$\cdots$	$\cdots$	$\cdots$	> 24	1800
e528.wcc5_3	$\cdots$	2003-11-28	Baade	N.S.	$\cdots$	$\cdots$	$\cdots$	$\cdots$	$\cdots$	$\cdots$	$\cdots$	> 24	$\cdots$
e529.wcc5_3	$\cdots$	2003-11-29.10	Clay	Unk	$\cdots$	$\cdots$	$\cdots$	$\cdots$	$\cdots$	$\cdots$	$\cdots$	> 24	3x1800
e531.wcc1_4	2003kv	2003-11-29.14	Baade	Ia?	$\cdots$	$\cdots$	0.79 (0.01)	$\cdots$	$\cdots$	$\cdots$	$\cdots$	23.1	3x1800
f001.wbb7_1	2003lg	2003-12-19.17	MMT	II	IIP	$\cdots$	0.173 (0.004)	2004et	24.0 (4.0)	$\cdots$	$\cdots$	> 24	3x1800
f011.wcc7_12	2003lh	2003-12-21.31	KI/LRIS	Ia	norm	$\cdots$	0.536 (0.006)	1990N	3.1 (1.8)	12.3 (1.8)	-0.090	22.7	1500
f017.wbb9_10	$\cdots$	2003-12-20.33	GMOS	AGN	$\cdots$	0.725	$\cdots$	$\cdots$	$\cdots$	$\cdots$	$\cdots$	22.1	3x1200
f041.wbb6_8	2003le	2003-12-20.23	KI/LRIS	Ia	norm	$\cdots$	0.558 (0.007)	1989B	1.9 (3.7)	7.8 (0.6)	-0.301	$\cdots$	2x1200
f044.wbb8_8	$\cdots$	2003-12-21.10	MMT	Gal	$\cdots$	0.409	$\cdots$	$\cdots$	$\cdots$	$\cdots$	$\cdots$	> 24	3x1800
f076.wbb9_01	2003lf	2003-12-21.29	KI/LRIS	Ia	norm	$\cdots$	0.411 (0.006)	1994D	1.2 (2.9)	4.6 (0.8)	0.175	$\cdots$	900
f076.wbb9_01	2003lf	2003-12-21.17	MMT	Ia	norm	$\cdots$	0.411 (0.006)	1994D	1.2 (2.9)	4.6 (0.8)	0.175	$\cdots$	3x900
f095.wcc2_8	$\cdots$	2003-12-20.31	KI/LRIS	Gal	$\cdots$	0.313	$\cdots$	$\cdots$	$\cdots$	$\cdots$	$\cdots$	23.6	3x1200
f096.waa3_3	2003lm	2003-12-21.28	KI/LRIS	Ia	$\cdots$	0.408	0.413 (0.004)	2003du	2.0 (1.6)	5.4 (2.0)	0.171	$\cdots$	1500
f116.wbb1_7	$\cdots$	2003-12-20	KI/LRIS	N.S.	$\cdots$	$\cdots$	$\cdots$	$\cdots$	$\cdots$	$\cdots$	$\cdots$	$\cdots$	$\cdots$
f123.wcc1_7	$\cdots$	2003-12-21.34	KI/LRIS	Ia?	$\cdots$	0.526	0.53 (0.01)	$\cdots$	$\cdots$	$\cdots$	$\cdots$	23.0	2x1200
f213.wbb4_12	$\cdots$	2003-12-19.34	GMOS	Unk	$\cdots$	$\cdots$	$\cdots$	$\cdots$	$\cdots$	$\cdots$	$\cdots$	22.6	2x1200
f216.wdd4_15	2003ll	2003-12-21.44	KI/LRIS	Ia	norm	0.596	0.595 (0.011)	2003cg	7.9 (4.7)	9.9 (0.8)	-0.104	$\cdots$	1800
f221.wcc4_14	2003lk	2003-12-21.36	KI/LRIS	Gal	$\cdots$	0.442	$\cdots$	$\cdots$	$\cdots$	$\cdots$	$\cdots$	$\cdots$	1500
f231.waa1_13	2003ln	2003-12-21.25	KI/LRIS	Ia	$\cdots$	$\cdots$	0.620 (0.008)	2001eh	5.0 (2.5)	9.4 (0.4)	-0.247	23.4	1500
f235.wbb5_13	2003lj	2003-12-20.27	KI/LRIS	Ia	$\cdots$	0.417	0.422 (0.006)	1994ae	3.3 (2.0)	5.1 (0.5)	0.165	21.6	2x1200
f244.wdd3_8	2003li	2003-12-20.42	KI/LRIS	Ia	norm	0.544	0.546 (0.005)	2005el	5.4 (2.5)	8.4 (1.6)	-0.020	22.7	2x1800
f301.wdd6_1	$\cdots$	2003-12-21.42	KI/LRIS	Ia	$\cdots$	$\cdots$	0.514 (0.011)	2006le	$\cdots$	$\cdots$	$\cdots$	$\cdots$	1500
f304.wdd6_2	$\cdots$	2003-12-21.39	KI/LRIS	Unk	$\cdots$	$\cdots$	$\cdots$	$\cdots$	$\cdots$	$\cdots$	$\cdots$	$\cdots$	1800
f308.wdd6_10	$\cdots$	2003-12-20.37	KI/LRIS	Ia	$\cdots$	$\cdots$	0.388 (0.010)	1999aa	$\cdots$	$\cdots$	$\cdots$	$\cdots$	3x1800
f441.wbb6_7	$\cdots$	2003-12-23.25	GMOS	Unk	$\cdots$	$\cdots$	$\cdots$	$\cdots$	$\cdots$	$\cdots$	$\cdots$	$\cdots$	3x1200
g001.waa1_1	2004fi	2004-10-18.489	KI/LRIS	Gal	$\cdots$	0.265	$\cdots$	$\cdots$	$\cdots$	$\cdots$	$\cdots$	$\cdots$	900
g004.wbb4_14	$\cdots$	2004-11-11.176	Clay	Ic	norm	$\cdots$	0.143 (0.006)	2004aw	$\cdots$	$\cdots$	$\cdots$	$\cdots$	2x600
g005.waa2_13	2004fh	2004-10-18.502	KI/LRIS	Ia	norm	$\cdots$	0.218 (0.007)	1998es	1.8 (0.8)	2.9 (0.4)	-0.253	$\cdots$	900
g009.wbb4_13	$\cdots$	2004-10-21.272	GMOS	Gal	$\cdots$	0.183	$\cdots$	$\cdots$	$\cdots$	$\cdots$	$\cdots$	$\cdots$	3x1800
g009.wbb4_13	$\cdots$	2004-11-11.119	Clay	Unk	$\cdots$	0.183	$\cdots$	$\cdots$	$\cdots$	$\cdots$	$\cdots$	$\cdots$	600
g014.wbb1_6	$\cdots$	2004-11-11.075	Clay	Unk	$\cdots$	0.195	$\cdots$	$\cdots$	$\cdots$	$\cdots$	$\cdots$	22.5	2x600
g043.wbb6_16	2004fj	2004-10-18.566	KI/LRIS	II	IIP	0.187	0.190 (0.002)	1999em	6.4 (2.3)	$\cdots$	$\cdots$	21.6	1800
g046.wcc9_14	$\cdots$	2004-12-17.177	Clay	Gal	$\cdots$	0.184	$\cdots$	$\cdots$	$\cdots$	$\cdots$	$\cdots$	20.6	3x600,2x600
g050.waa7_10	2004fn	2004-10-21.158	GMOS	Ia	norm	0.605	0.616 (0.008)	2003du	-4.4 (2.9)	-1.6 (0.6)	-0.318	23.5	3x1800
g052.waa8_7	2004fm	2004-10-18.393	KI/LRIS	Ia	norm	$\cdots$	0.384 (0.006)	2002ha	2.8 (2.2)	0.5 (0.4)	0.382	22.5	1800
g053.waa8_7	2004fl	2004-10-18.393	KI/LRIS	Ia?	$\cdots$	0.632	$\cdots$	$\cdots$	$\cdots$	$\cdots$	$\cdots$	22.8	1800
g055.wbb7_7	2004fk	2004-10-17.373	GMOS	Ia	norm	0.296	0.302 (0.006)	2002er	5.3 (1.7)	6.8 (1.1)	-0.294	22.3	4x1800
g097.waa8_16	$\cdots$	2004-11-03.055	Clay	Ia	norm	0.343	0.339 (0.004)	1994D	11.9 (1.7)	14.3 (0.4)	-0.289	23.1	1200, 1800
g108.wdd8_4	2004fp	2004-10-17.489	GMOS	II	IIP	$\cdots$	0.162 (0.004)	1992H	49.0 (36.7)	$\cdots$	$\cdots$	22.1	3x1800
g120.wbb1_1	2004fo	2004-10-18.528	KI/LRIS	Ia	$\cdots$	$\cdots$	0.506 (0.007)	1999aw	-1.1 (4.7)	-1.4 (0.7)	-0.286	22.3	1800
g128.waa2_5	$\cdots$	2004-11-10.271	GMOS	II?	$\cdots$	0.164	$\cdots$	$\cdots$	$\cdots$	$\cdots$	$\cdots$	23.5	5x1800
g133.wcc4_7	$\cdots$	2004-11-09.428	GMOS	Ia	norm	$\cdots$	0.420 (0.002)	2006ac	37.9 (5.1)	27.8 (1.9)	-0.351	21.8	5x1800
g142.waa2_11	$\cdots$	2004-11-06.028	Clay	Ia	$\cdots$	0.404	0.398 (0.001)	1994Q	$\cdots$	19.7 (0.8)	0.210	22.9	2x1200

TABLE 2 — *Continued*

ESSENCE ID[a]	IAUC ID[b]	UT Date	Telescope	Type[c]	Subtype	z (Gal)[d]	z (SNID)[e]	Template	Phase (SNID) (d)	Phase (LC) (d)	Δ	Disc. Mag.	Exp. (s)
g151.waa2_14	2004fq	2004-10-18.443	KI/LRIS	Gal	$\cdots$	0.146	$\cdots$	$\cdots$	$\cdots$	$\cdots$	$\cdots$	21.3	1200
g160.wdd8_15	2004fs	2004-10-19.535	GMOS	Ia	$\cdots$	$\cdots$	0.507 (0.019)	1997br	$\cdots$	14.6 (0.6)	-0.308	22.4	3x1800
g166.wdd9_14	2004fr	2004-10-18.593	KI/LRIS	Gal	$\cdots$	0.202	$\cdots$	$\cdots$	$\cdots$	$\cdots$	$\cdots$	22.1	2000+1800
g181.wdd9_2	$\cdots$	2004-11-11.154	Clay	Unk	$\cdots$	0.533	$\cdots$	$\cdots$	$\cdots$	$\cdots$	$\cdots$	22.7	3x600
g185.waa2_1	$\cdots$	2004-10-18.448	KI/LRIS	II	IIP	$\cdots$	0.330 (0.005)	1999em	11.1 (12.8)	$\cdots$	$\cdots$	23.3	2400,2x1200
g199.wdd4_7	2004ft	2004-10-18.621	KI/LRIS	Gal	$\cdots$	0.766	$\cdots$	$\cdots$	$\cdots$	$\cdots$	$\cdots$	23.0	2100
g204.wcc2_13	$\cdots$	2004-11-11.099	Clay	Unk	$\cdots$	0.114	$\cdots$	$\cdots$	$\cdots$	$\cdots$	$\cdots$	> 24	3x600
g213.wbb8_6	$\cdots$	2004-11-11.197	GMOS	Gal	$\cdots$	0.843	$\cdots$	$\cdots$	$\cdots$	$\cdots$	$\cdots$	22.8	3x1800
g219.wbb9_10	$\cdots$	2004-11-19.090	GMOS	II?	$\cdots$	$\cdots$	$\cdots$	$\cdots$	$\cdots$	$\cdots$	$\cdots$	22.4	5x1800
g225.waa5_2	$\cdots$	2004-11-08.282	GMOS	Ia	norm	$\cdots$	0.579 (0.009)	1994T	$\cdots$	$\cdots$	$\cdots$	> 24	4x1800
g230.wbb5_5	$\cdots$	2004-11-14.313	KI/LRIS	Ia	$\cdots$	0.392	0.394 (0.001)	1999aw	5.1 (3.7)	$\cdots$	$\cdots$	22.8	1200
g240.waa1_14	$\cdots$	2004-11-14.276	KI/LRIS	Ia	norm	$\cdots$	0.689 (0.005)	1994ae	10.1 (1.0)	16.3 (0.7)	-0.163	24.0	1800
g276.wcc1_7	$\cdots$	2004-12-16.152	Clay	Gal	$\cdots$	0.000	$\cdots$	$\cdots$	$\cdots$	$\cdots$	$\cdots$	21.6	1200
h280.wbb6_10	$\cdots$	2004-11-14.296	KI/LRIS	II	IIL	0.262	0.252 (0.001)	1990K	$\cdots$	$\cdots$	$\cdots$	21.5	1200
h283.wcc9_5	2004ha	2004-11-14.335	KI/LRIS	Ia	norm	$\cdots$	0.495 (0.007)	1993ac	4.9 (3.0)	2.2 (1.1)	0.090	22.5	1800
h293.wcc9_2	$\cdots$	2004-11-14.360	KI/LRIS	Unk	$\cdots$	0.546	$\cdots$	$\cdots$	$\cdots$	$\cdots$	$\cdots$	23.4	1800
h296.wdd6_12	$\cdots$	2004-11-11.057	Clay	Gal	$\cdots$	0.059	$\cdots$	$\cdots$	$\cdots$	$\cdots$	$\cdots$	> 24	600
h299.wcc8_15	2004hb	2004-11-11.366	GMOS	Gal	$\cdots$	0.720	$\cdots$	$\cdots$	$\cdots$	$\cdots$	$\cdots$	23.9	4x1800
h300.wdd8_15	$\cdots$	2004-11-14.532	KI/LRIS	Ia	norm	$\cdots$	0.656 (0.001)	1993ac	$\cdots$	14.4 (0.7)	-0.279	23.2	1800
h304.wcc1_2	$\cdots$	2004-12-01.083	Baade	Gal	$\cdots$	$\cdots$	$\cdots$	$\cdots$	$\cdots$	$\cdots$	$\cdots$	22.1	2x600
h311.waa3_4	2004hc	2004-11-14.249	KI/LRIS	Ia	$\cdots$	$\cdots$	0.760 (0.009)	1999ac	7.7 (4.1)	10.6 (0.7)	-0.491	24.1	1800
h317.wcc8_10	$\cdots$	2005-10-07.192	Clay	Gal	$\cdots$	0.638	$\cdots$	$\cdots$	$\cdots$	$\cdots$	$\cdots$	23.4	3x1200
h319.wcc5_11	2004hd	2004-11-18.233	GMOS	Ia	norm	0.490	0.478 (0.002)	2006ax	-2.5 (3.2)	-8.5 (0.5)	-0.274	22.4	3x1800
h323.wdd6_13	2004he	2004-11-17.199	GMOS	Ia	norm	0.598	0.603 (0.007)	2002bo	-1.4 (3.1)	-1.2 (0.6)	-0.108	> 24	5x1800
h342.wdd5_9	2004hf	2004-12-03.155	Baade	Ia	norm	$\cdots$	0.421 (0.005)	2006le	7.8 (1.5)	16.7	-0.356	> 24	4x600
h345.wdd4_10	2004hg	2004-12-02.138	Baade	Unk	$\cdots$	$\cdots$	$\cdots$	$\cdots$	$\cdots$	$\cdots$	$\cdots$	22.7	4x600
h352.wcc4_13	$\cdots$	2004-12-16.080	Clay	Gal	$\cdots$	0.181	$\cdots$	$\cdots$	$\cdots$	$\cdots$	$\cdots$	21.8	1200
h353.waa2_15	$\cdots$	2004-12-16.058	Clay	Gal	$\cdots$	0.219	$\cdots$	$\cdots$	$\cdots$	$\cdots$	$\cdots$	23.0	2x600
h359.wcc8_10	2004hi	2004-12-17.092	Clay	Ia	norm	$\cdots$	0.348 (0.005)	2003du	8.9 (1.7)	15.3 (0.4)	-0.182	23.9	2x1200
h361.wcc7_13	$\cdots$	2004-12-16	Clay	Unk	$\cdots$	$\cdots$	$\cdots$	$\cdots$	$\cdots$	$\cdots$	$\cdots$	22.7	no spec
h363.wcc9_16	2004hh	2004-12-03.084	Baade	Ia	norm	$\cdots$	0.211 (0.005)	1994M	6.0 (1.8)	4.6 (0.3)	0.065	22.5	3x1000
h364.wdd9_13	2004hj	2004-12-01.121	Baade	Ia	norm	$\cdots$	0.344 (0.004)	1994ae	2.3 (1.6)	7.6 (0.4)	-0.006	22.7	2x600
k374.wdd9_1	$\cdots$	2004-12-09.143	Baade	Unk	$\cdots$	0.143	$\cdots$	$\cdots$	$\cdots$	$\cdots$	$\cdots$	22.1	540+450
k374.wdd9_1	$\cdots$	2005-01-09.111	Clay	Gal	$\cdots$	0.143	$\cdots$	$\cdots$	$\cdots$	$\cdots$	$\cdots$	22.1	3x1200
k396.waa2_5	2004hk	2004-12-10.096	Baade	Ia?	$\cdots$	0.262	$\cdots$	$\cdots$	$\cdots$	-6.0 (0.4)	0.843	22.3	2x450
k397.wcc1_7	$\cdots$	2004-12-16.115	Clay	Ic	norm	$\cdots$	0.051 (0.003)	$\cdots$	$\cdots$	$\cdots$	$\cdots$	23.4	3x1200
k397.wcc1_7	$\cdots$	2004-12-17.152	Clay	Ic	norm	$\cdots$	0.051 (0.003)	$\cdots$	$\cdots$	$\cdots$	$\cdots$	23.4	2x1200
k402.wbb5_12	$\cdots$	2004-12-15.334	KII/DEIMOS	Unk	$\cdots$	$\cdots$	$\cdots$	$\cdots$	$\cdots$	$\cdots$	$\cdots$	> 24	2400
k411.waa3_10	$\cdots$	2004-12-12.244	KI/LRIS	Ia	$\cdots$	$\cdots$	0.565 (0.003)	1999cc	5.2 (2.2)	$\cdots$	$\cdots$	22.2	1500
k420.wdd6_13	$\cdots$			$\cdots$	$\cdots$	$\cdots$	$\cdots$	$\cdots$	$\cdots$	$\cdots$	$\cdots$	22.2	
k425.wbb7_3	2004hl	2004-12-09.087	Baade	Ia	norm	0.270	0.274 (0.003)	1998dm	10.8 (2.1)	14.1 (0.3)	-0.021	21.5	3x600
k429.wdd3_6	2004hm	2004-12-09.181	Baade	Ia	$\cdots$	0.172	0.171 (0.006)	2003hu	0.8 (1.1)	-1.2 (0.4)	-0.094	20.2	2x450
k430.wbb1_2	2004hn	2004-12-12.311	KI/LRIS	Ia	norm	$\cdots$	0.576 (0.007)	2002er	2.2 (2.6)	1.4 (1.2)	-0.112	> 24	2x1800
k432.waa2_3	$\cdots$	2004-12-12.271	KI/LRIS	Ia	norm	$\cdots$	0.706 (0.010)	1999ee	$\cdots$	$\cdots$	$\cdots$	23.3	2400
k437.wcc3_11	2004ho	2004-12-10.160	Baade	Gal	$\cdots$	0.288	$\cdots$	$\cdots$	$\cdots$	$\cdots$	$\cdots$	> 24	3x600
k440.wbb4_7	$\cdots$	2004-12-12.365	KI/LRIS	Unk	$\cdots$	$\cdots$	$\cdots$	$\cdots$	$\cdots$	$\cdots$	$\cdots$	> 24	2x1800
k441.wdd5_5	2004hq	2004-12-16.375	GMOS	Ia	$\cdots$	$\cdots$	0.671 (0.007)	1999aw	-1.1 (5.5)	4.0 (1.3)	-0.203	24.4	4x1800
k442.wcc3_10	$\cdots$	2004-12-12.449	KI/LRIS	Unk	$\cdots$	$\cdots$	$\cdots$	$\cdots$	$\cdots$	$\cdots$	$\cdots$	> 24	1800
k443.wcc1_4	2004hp	2004-12-12.417	KI/LRIS	Unk	$\cdots$	$\cdots$	$\cdots$	$\cdots$	$\cdots$	$\cdots$	$\cdots$	23.2	1800+1400
k444.wdd5_2	$\cdots$	2005-01-09.149	Clay	Gal	$\cdots$	0.193	$\cdots$	$\cdots$	$\cdots$	$\cdots$	$\cdots$	> 24	1200
k448.wbb6_2	2004hr	2004-12-17.055	Clay	Ia	norm	0.409	0.405 (0.007)	2002er	-2.5 (2.2)	1.5 (1.2)	0.003	22.5	2x1200+188
k459.wcc7_10	$\cdots$	2004-12-18.055	Clay	Unk	$\cdots$	$\cdots$	$\cdots$	$\cdots$	$\cdots$	$\cdots$	$\cdots$	> 24	3x1200
k467.wdd2_13	$\cdots$	2004-12-15.414	KII/DEIMOS	Unk	$\cdots$	$\cdots$	$\cdots$	$\cdots$	$\cdots$	$\cdots$	$\cdots$	> 24	2800
k472.wcc3_15	$\cdots$	2005-01-10.089	Clay	Gal	$\cdots$	0.138	$\cdots$	$\cdots$	$\cdots$	$\cdots$	$\cdots$	20.8	2x1200
k485.wcc4_6	2004hs	2004-12-18.125	Clay	Ia	$\cdots$	$\cdots$	0.422 (0.007)	1999ee	2.5 (1.6)	8.2 (1.1)	-0.230	> 24	4x1200

TABLE 2 — *Continued*

ESSENCE ID[a]	IAUC ID[b]	UT Date	Telescope	Type[c]	Subtype	z (Gal)[d]	z (SNID)[e]	Template	Phase (SNID) (d)	Phase (LC) (d)	Δ	Disc. Mag.	Exp. (s)
k490.wdd2_4	⋯	2004-12-15.377	KII/DEIMOS	Ia	norm	0.716	0.709 (0.001)	1996X	⋯	⋯	⋯	24.4	3000
k505.wcc3_13	⋯	2005-01-09.061	Clay	Gal	⋯	0.241	⋯	⋯	⋯	⋯	⋯	22.0	3x1200
k505.wcc3_13	⋯	2005-10-07.141	Clay	Gal	⋯	0.241	⋯	⋯	⋯	⋯	⋯	22.0	2x1200
k509.waa5_10	⋯	2005-10-07.106	Clay	Gal	⋯	0.207	⋯	⋯	⋯	⋯	⋯	21.8	2x1200
m001.wbb6_1	⋯	2005-10-05.131	Clay	Ia	norm	⋯	0.287 (0.004)	2006lf	11.9 (2.1)	⋯	⋯	⋯	2x1200
m001.wbb6_1	⋯	2005-10-05.432	KII/DEIMOS	Ia	norm	⋯	0.287 (0.004)	2006lf	11.9 (2.1)	⋯	⋯	⋯	2x1800
m002.waa6_15	⋯	2005-10-04.090	VLT	Gal	⋯	0.354	⋯	⋯	⋯	⋯	⋯	⋯	2x1800
m003.wcc9_15	⋯	2005-10-04.229	VLT	II	IIP	0.201	0.203 (0.005)	2004dj	17.0 (11.8)	⋯	⋯	⋯	2x1200
m004.wcc8_8	⋯	2005-10-06.147	VLT	Gal	⋯	0.384	⋯	⋯	⋯	⋯	⋯	⋯	1800
m006.wdd8_1	⋯	2005-10-04.382	VLT	Ia	⋯	0.057	⋯	⋯	⋯	⋯	⋯	⋯	900
m006.wdd8_1	⋯	2005-10-05.266	Clay	Ic	norm	0.057	0.050 (0.002)	2004gk	35.7 (27.7)	⋯	⋯	⋯	3x900+300
m006.wdd8_1	⋯	2005-10-06.603	KII/DEIMOS	II	IIn	0.057	0.050 (0.004)	1997cy	⋯	⋯	⋯	⋯	2x1200
m006.wdd8_1	⋯	2005-10-07.564	KI/LRIS	II	IIn	0.057	0.050 (0.004)	1997cy	⋯	⋯	⋯	⋯	1500
m010.wdd8_9	⋯	2005-10-05.320	VLT	Ib	IIb	0.216	0.217 (0.003)	1996cb	32.8 (5.7)	⋯	⋯	23.1	2x1800
m011.wcc5_16	⋯	2005-10-04.215	VLT	II	⋯	0.205	⋯	⋯	⋯	⋯	⋯	20.2	1800
m012.wdd3_16	⋯	2005-10-04.274	VLT	Gal	⋯	0.114	⋯	⋯	⋯	⋯	⋯	21.4	2x1200
m014.wcc5_3	⋯	2005-10-05.212	VLT	II	IIP	0.199	0.200 (0.004)	2006bp	24.6 (12.7)	⋯	⋯	22.9	2x1800
m022.waa1_14	⋯	2005-10-05.094	VLT	Ia	norm	⋯	0.240 (0.003)	2003du	38.8 (8.8)	10.8 (1.8)	−0.727	22.1	2x1800
m025.waa6_11	⋯	2005-10-05.276	KII/DEIMOS	Gal	⋯	0.701	⋯	⋯	⋯	⋯	⋯	21.7	3x1800
m026.waa5_12	⋯	2005-10-05.347	KII/DEIMOS	Ia	norm	0.655	0.656 (0.006)	1999ao	7.6 (3.8)	20.0 (1.8)	−0.201	23.2	3x1800
m026.waa5_12	⋯	2005-10-07.304	KI/LRIS	Ia	norm	0.655	0.656 (0.006)	1999ao	7.6 (3.8)	22.0 (1.8)	−0.201	23.2	6x1800
m027.wbb6_12	⋯	2005-10-04.146	VLT	Ia	norm	0.289	0.285 (0.004)	1999bk	6.4 (2.3)	8.8 (1.1)	−0.134	21.9	1800+100
m027.wbb6_12	⋯	2005-10-07.406	KI/LRIS	Ia	norm	0.289	0.286 (0.005)	1994ae	8.9 (1.7)	11.8 (1.1)	−0.134	21.9	3x1800
m028.wcc5_12	⋯	2005-10-06.509	KII/DEIMOS	Gal	⋯	0.606	⋯	⋯	⋯	⋯	⋯	21.5	1200,1180
m032.waa7_2	⋯	2005-10-06.051	Clay	Ia	norm	⋯	0.155 (0.003)	1995D	15.8 (2.3)	18.3 (1.8)	−0.158	20.4	3x1200
m034.wdd3_2	⋯	2005-10-04.384	VLT	Ia	norm	0.558	0.566 (0.007)	1992A	⋯	14.6 (1.9)	−0.087	22.8	2x1200
m035.waa1_5	⋯	2005-10-05.366	VLT	AGN	⋯	⋯	⋯	⋯	⋯	⋯	⋯	22.7	3x1800
m037.wdd3_10	⋯	2005-10-05.253	VLT	Gal	⋯	0.240	⋯	⋯	⋯	⋯	⋯	22.4	1800+1200
m038.wcc9_6	⋯	2005-10-06.283	VLT	II	IIP	0.051	0.051 (0.003)	1992H	146.9 (46.0)	⋯	⋯	20.6	1200
m039.wdd3_6	⋯	2005-10-05.377	VLT	Ia	⋯	0.248	0.247 (0.003)	1998eg	20.8 (2.8)	21.3 (1.9)	−0.223	21.2	1800
m039.wdd3_6	⋯	2005-10-05.562	KII/DEIMOS	Ia	⋯	0.248	0.247 (0.003)	1998eg	20.8 (2.8)	21.3 (1.9)	−0.223	21.2	3x1800
m040.wdd3_6	⋯	2005-10-05.562	KII/DEIMOS	Ia	norm	⋯	0.480 (0.004)	1998dk	18.1 (2.0)	21.3 (1.9)	⋯	21.2	3x1800
m041.wcc7_7	⋯	2005-10-06.331	VLT	II	IIP	⋯	0.220 (0.005)	2006bp	20.0 (15.1)	⋯	⋯	22.8	1800+998
m042.waa6_3	⋯	2005-10-04.035	VLT	Unk	⋯	0.126	⋯	⋯	⋯	⋯	⋯	21.8	2x1200
m042.waa6_3	⋯	2005-10-07.049	Clay	Unk	⋯	0.126	⋯	⋯	⋯	⋯	⋯	21.8	4x1200
m043.waa1_1	⋯	2005-10-05.122	VLT	Ia	norm	0.265	0.266 (0.003)	1999X	25.9 (2.7)	14.9 (2.0)	−0.466	21.9	1800
m057.wcc4_11	⋯	2005-10-06.188	VLT	Ia	⋯	0.181	0.183 (0.004)	1999aa	45.3 (2.3)	17.0 (2.1)	−0.601	21.7	1800
m062.wbb3_10	⋯	2005-10-06.476	KII/DEIMOS	Ia	norm	0.314	0.316 (0.004)	2003cg	2.5 (0.8)	4.9 (1.1)	0.149	21.5	2x1200
m070.wdd4_7	⋯	2005-10-05.613	KII/DEIMOS	Ia	norm	0.212	0.214 (0.003)	2003du	9.8 (0.9)	⋯	⋯	20.6	1200,1118
m075.waa3_7	⋯	2005-10-04.179	VLT	Ia	norm	0.100	0.101 (0.003)	1998ec	27.0 (8.1)	2.4 (1.9)	−0.387	19.0	1800+30
m075.waa3_7	⋯	2005-10-05.069	Clay	Ia	norm	0.100	0.101 (0.003)	1998ec	27.0 (8.1)	3.4 (1.9)	−0.387	19.0	3x900
m078.wcc2_5	⋯	2005-10-05.169	VLT	Gal	⋯	0.395	⋯	⋯	⋯	⋯	⋯	22.1	1800
m082.wcc2_4	⋯	2005-10-05.491	KII/DEIMOS	Unk	⋯	⋯	⋯	⋯	⋯	⋯	⋯	22.6	2x1800,786
m087.wdd4_3	⋯	2005-10-05.395	VLT	Ia	⋯	0.287	0.289 (0.006)	1995E	7.1 (2.6)	⋯	⋯	21.5	1500
m095.wdd2_3	⋯	2005-10-04.339	VLT	AGN	⋯	0.990	⋯	⋯	⋯	⋯	⋯	22.6	3x1200
m111.wcc7_11	⋯	2005-10-06.547	KII/DEIMOS	AGN	⋯	1.000	⋯	⋯	⋯	⋯	⋯	21.9	1800,1400
m135.waa1_2	⋯	2005-10-06.232	VLT	Gal	⋯	0.289	⋯	⋯	⋯	⋯	⋯	21.5	1800+774
m135.waa1_2	⋯	2005-10-06.257	KII/DEIMOS	Unk	⋯	0.289	⋯	⋯	⋯	⋯	⋯	21.5	2x1800
m138.wbb3_3	⋯	2005-10-06.256	VLT	Ia	norm	0.588	0.584 (0.007)	2002er	−5.8 (2.0)	−10.3 (1.3)	−0.306	22.6	1800
m138.wbb3_3	⋯	2005-10-06.372	KII/DEIMOS	Ia	norm	0.588	0.584 (0.007)	2002er	−5.8 (2.0)	−10.3 (1.3)	−0.306	22.6	5x1800
m138.wbb3_3	⋯	2005-10-07.495	KI/LRIS	Ia	norm	0.588	0.584 (0.007)	2002er	−5.8 (2.0)	−9.3 (1.3)	−0.306	22.6	5x1800
m139.waa3_7	⋯	2005-10-06.300	KII/DEIMOS	II	IIn	0.212	0.204 (0.001)	2000eo	18.5 (12.0)	⋯	⋯	22.7	1800,900
m142.wbb1_12	⋯	2005-10-06.447	KII/DEIMOS	N.S.	⋯	0.597	⋯	⋯	⋯	⋯	⋯	20.8	2x900
m158.waa6_3	⋯	2005-10-28.056	Clay	Ia	norm	⋯	0.461 (0.007)	2004eo	21.7 (16.7)	15.5 (1.2)	−0.334	22.6	2x1200
m158.waa6_3	⋯	2005-10-29.087	Clay	Ia	norm	⋯	0.461 (0.007)	2004eo	21.7 (16.7)	16.5 (1.2)	−0.334	22.6	3x1200

TABLE 2 — *Continued*

ESSENCE ID[a]	IAUC ID[b]	UT Date	Telescope	Type[c]	Subtype	z (Gal)[d]	z (SNID)[e]	Template	Phase (SNID) (d)	Phase (LC) (d)	Δ	Disc. Mag.	Exp. (s)
m158.waa6_3	⋯	2005-10-30.167	GMOS	Ia	norm	⋯	0.461 (0.007)	2004eo	21.7 (16.7)	17.5 (1.2)	−0.334	22.6	5x1800
m161.wdd9_4	⋯	2005-10-28.149	Clay	Gal	⋯	0.230	⋯	⋯	⋯	⋯	⋯	22.8	1200
m166.waa1_5	⋯	2005-10-28.354	GMOS	AGN	⋯	0.303	⋯	⋯	⋯	⋯	⋯	23.0	5x1800
m193.wdd3_14	⋯	2005-10-28.104	Clay	Ia	norm	0.330	0.336 (0.006)	1996X	6.4 (3.2)	9.2 (0.5)	−0.124	21.8	2x1200
m193.wdd3_14	⋯	2005-10-29.135	Clay	Ia	norm	0.330	0.336 (0.006)	1996X	6.4 (3.2)	10.2 (0.5)	−0.124	21.8	3x1200
m226.wcc9_16	⋯	2005-10-31.274	GMOS	Ia	⋯	0.675	0.674 (0.008)	2006X	⋯	23.5 (1.2)	−0.227	22.9	4x1800
n244.wdd3_7	⋯	2005-12-05.341	KI/LRIS	Unk	⋯	⋯	⋯	⋯	⋯	⋯	⋯	22.1	2x1800
n244.wdd3_7	⋯	2006-01-07.161	Baade	Unk	⋯	⋯	⋯	⋯	⋯	⋯	⋯	22.1	2x600
n246.wbb7_11	⋯	2005-12-02.191	VLT	Ia?	⋯	0.705	0.71 (0.01)	⋯	⋯	⋯	⋯	22.8	3x1200
n255.wcc7_5	⋯	2006-01-07.099	Baade	Gal	⋯	⋯	⋯	⋯	⋯	⋯	⋯	22.9	2x1200
n256.wdd3_5	⋯	2005-12-02.277	VLT	Ia	norm	⋯	0.630 (0.011)	2003du	2.0 (1.6)	10.2 (0.9)	−0.339	22.6	2x1200
n258.wcc5_4	⋯	2005-12-02.232	VLT	Ia	norm	0.519	0.525 (0.008)	1992A	8.5 (2.6)	9.3 (1.2)	0.032	22.4	900
n260.wcc8_2	⋯	2005-12-02.131	GMOS	AGN	⋯	2.000	⋯	⋯	⋯	⋯	⋯	23.1	5x1800
n261.wbb7_16	⋯	2005-11-30.326	GMOS	AGN	⋯	3.500	⋯	⋯	⋯	⋯	⋯	22.5	5x1800
n263.wcc9_4	⋯	2005-12-02.211	VLT	Ia	⋯	⋯	0.368 (0.007)	1999aw	4.8 (4.4)	4.0 (0.5)	0.054	21.5	900+286
n268.wdd6_15	⋯	2005-12-04.252	VLT	Unk	⋯	0.279	⋯	⋯	⋯	⋯	⋯	22.6	2x1800
n271.wbb5_16	⋯	2005-12-02.376	KII/DEIMOS	II	IIP	⋯	0.242 (0.005)	1999em	17.1 (10.2)	⋯	⋯	22.0	4x900
n278.waa5_11	⋯	2005-12-03.040	VLT	Ia	norm	0.303	0.308 (0.006)	1995E	2.6 (2.1)	7.8 (0.9)	0.033	21.5	2x900
n284.waa1_8	⋯	2005-11-29.298	GMOS	AGN	⋯	1.980	⋯	⋯	⋯	⋯	⋯	22.3	4x1800
n285.waa3_8	⋯	2005-12-04.098	VLT	Ia	norm	0.533	0.531 (0.009)	2004S	16.1 (4.5)	21.0 (1.3)	−0.122	22.6	2x1800
n295.waa3_3	⋯	2005-11-29.083	GMOS	AGN	⋯	1.240	⋯	⋯	⋯	⋯	⋯	22.5	2x1800
n295.waa3_3	⋯	2005-11-30.084	GMOS	AGN	⋯	1.240	⋯	⋯	⋯	⋯	⋯	22.5	3x1800
n296.wbb5_3	⋯	2006-01-07.074	Baade	Unk	⋯	⋯	⋯	⋯	⋯	⋯	⋯	21.7	2x900
n312.wdd9_14	⋯	2005-12-02.432	KII/DEIMOS	Gal	⋯	0.286	⋯	⋯	⋯	⋯	⋯	22.0	4x900
n322.wdd9_12	⋯	2005-12-04.397	KI/LRIS	Ia	norm	⋯	0.770 (0.010)	1994S	⋯	⋯	⋯	23.6	2x1600
n326.waa1_10	⋯	2005-12-02.067	VLT	Ia	norm	0.264	0.267 (0.006)	2006lf	−0.8 (3.6)	−3.0 (0.4)	0.703	21.7	2x1200
n346.waa1_3	⋯	2005-12-04.246	KI/LRIS	Gal	⋯	0.266	⋯	⋯	⋯	⋯	⋯	22.6	2x1200
n368.waa7_9	⋯	2005-12-03.118	VLT	Ia	norm	0.342	0.342 (0.006)	2005am	2.4 (1.9)	⋯	⋯	> 24	2x900
n395.wcc8_7	⋯	2005-12-03.414	KII/DEIMOS	Gal	⋯	0.462	⋯	⋯	⋯	⋯	⋯	21.9	1500
n400.wbb8_12	⋯	2005-12-04.319	KI/LRIS	Ia	norm	0.424	0.421 (0.007)	1999cl	−3.4 (2.9)	⋯	⋯	23.6	2x1200
n404.wdd8_14	⋯	2005-12-03.254	VLT	Ia	norm	⋯	0.211 (0.005)	2006ax	−7.8 (2.2)	−5.0 (0.4)	−0.069	21.8	860
n406.wdd8_16	⋯	2005-12-04.205	VLT	Ia?	⋯	⋯	0.770 (0.010)	⋯	⋯	⋯	⋯	23.4	2x1800
n406.wdd8_16	⋯	2005-12-05.139	VLT	Ia?	⋯	⋯	0.775 (0.010)	⋯	⋯	⋯	⋯	23.4	2x1800
n408.wbb9_16	⋯	2005-12-05.221	KI/LRIS	Unk	⋯	⋯	⋯	⋯	⋯	⋯	⋯	24.0	1800
p415.waa3_16	⋯	2005-12-04.052	VLT	Gal	⋯	0.343	⋯	⋯	⋯	⋯	⋯	21.8	900
p425.waa1_14	⋯	2005-12-02.100	VLT	Ia	norm	0.458	0.461 (0.009)	2006le	5.5 (2.8)	12.5 (0.8)	0.183	22.8	2x1200
p425.waa1_14	⋯	2005-12-03.273	KII/DEIMOS	Ia	norm	0.458	0.461 (0.009)	2006le	5.5 (2.8)	13.5 (0.8)	0.183	22.8	3x1200
p429.waa3_13	⋯	2005-12-02.141	VLT	Gal	⋯	0.548	⋯	⋯	⋯	⋯	⋯	23.3	2x1200
p429.waa3_13	⋯	2005-12-03.225	KII/DEIMOS	Gal	⋯	0.548	⋯	⋯	⋯	⋯	⋯	23.3	2x1200
p434.wbb5_12	⋯	2005-12-04.158	VLT	Ib/c	⋯	0.338	⋯	⋯	⋯	⋯	⋯	23.4	2x1800
p444.wcc2_5	⋯	2005-12-03.373	KII/DEIMOS	Ia	norm	⋯	0.633 (0.004)	2004dt	⋯	⋯	⋯	23.2	3x1200
p445.wbb1_4	⋯	2005-12-03.323	KII/DEIMOS	Ia	norm	0.807	0.816 (0.002)	2002bo	⋯	⋯	⋯	23.3	3x1200
p454.wcc2_15	⋯	2005-12-03.167	VLT	Ia	⋯	⋯	0.691 (0.009)	1999aw	3.1 (2.8)	3.8 (1.3)	−0.276	22.9	2x1800
p455.wcc4_15	⋯	2005-12-03.255	VLT	Ia	norm	0.297	0.285 (0.006)	1998dh	−7.9 (1.1)	−13.3 (0.4)	−0.061	21.4	2x900
p458.waa3_10	⋯	2005-12-05.197	KI/LRIS	Unk	⋯	⋯	⋯	⋯	⋯	⋯	⋯	23.1	1800
p459.wcc4_10	⋯	2005-12-03.210	VLT	Ia	⋯	⋯	0.702 (0.004)	1999dq	−5.2 (2.1)	⋯	⋯	23.2	2x1800
p461.waa5_6	⋯	2005-12-03.066	VLT	Gal	⋯	0.407	⋯	⋯	⋯	⋯	⋯	22.8	1800
p520.wcc2_12	⋯	2005-12-27.147	Clay	Ia?	⋯	0.643	⋯	⋯	⋯	⋯	⋯	23.0	3x1200
p520.wcc2_12	⋯	2005-12-28.094	Clay	Ia?	⋯	0.643	⋯	⋯	⋯	⋯	⋯	23.0	4x1200
p521.wcc7_14	⋯	2005-12-27.085	Clay	Gal	⋯	⋯	⋯	⋯	⋯	⋯	⋯	21.5	2x1200
p524.wdd8_6	⋯	2005-12-28.160	Clay	Ia	norm	⋯	0.511 (0.003)	2004eo	5.3 (2.3)	14.2 (0.4)	−0.229	22.6	4x1200
p527.wcc2_15	⋯	2005-12-29.142	Clay	Gal	⋯	0.435	⋯	⋯	⋯	⋯	⋯	22.4	3x1200
p527.wcc2_15	⋯	2006-01-01.371	KII/DEIMOS	Ia?	⋯	0.435	⋯	⋯	⋯	⋯	⋯	22.4	917
p528.wcc2_8	⋯	2005-12-29.092	Clay	Ia	⋯	0.782	⋯	⋯	⋯	7.6 (0.9)	−0.310	23.2	3x1200
p528.wcc2_8	⋯	2006-01-01.348	KII/DEIMOS	Ia	⋯	0.782	0.780 (0.009)	2002ha	3.4 (1.8)	10.6 (0.9)	−0.310	23.2	2x1800

TABLE 2 — *Continued*

ESSENCE ID[a]	IAUC ID[b]	UT Date	Telescope	Type[c]	Subtype	z (Gal)[d]	z (SNID)[e]	Template	Phase (SNID) (d)	Phase (LC) (d)	Δ	Disc. Mag.	Exp. (s)
p534.wcc3_4	⋯	2006-01-01.300	KII/DEIMOS	Ia	91T	0.621	0.612 (0.007)	1998es	0.8 (1.8)	−5.3	−0.096	22.7	2x2400
p534.wcc3_4	⋯	2006-01-03.072	GMOS	Ia	91T	0.621	0.612 (0.007)	1998es	0.8 (1.8)	−3.3	−0.096	22.7	5x1800

[a] ESSENCE internal identification. The first letter indicates the month in the observing season. This is followed by a sequential number as targets are discovered. The remaining letters and numbers show the specific ESSENCE field where the object was located. [b] Note that not all objects judged to be SNe have official International Astronomical Union names. [c] Our best guess as to classification of the object. Ia? indicates a lack of certainty in the identification as a SN Ia. Objects marked "Unk" are unknown. N.S. indicates that the telescope was pointed to the object, but no exposure was taken or the exposure contained no signal. [d] Redshift measured from narrow emission or absorption lines from the host galaxy. All galactic redshift errors are < 0.001. [e] Redshift measured from the SN spectrum by SNID.